

Interplay between k -core and community structure in complex networks

Irene Malvestio¹, Alessio Cardillo^{2,1,3,*}, and Naoki Masuda^{4,5,1,*}

¹Department of Engineering Mathematics, University of Bristol, Bristol, BS8 1UB, United Kingdom

²Department of Computer Science and Mathematics, University Rovira i Virgili, E-43007 Tarragona, Spain

³GOTHAM Lab – Institute for Biocomputation and Physics of Complex Systems (BIFI), University of Zaragoza, E-50018 Zaragoza, Spain

⁴Department of Mathematics, University at Buffalo, Buffalo, NY, 14260-2900, United States

⁵Computational and Data-Enabled Science and Engineering Program, University at Buffalo, State University of New York, Buffalo, NY 14260-5030, USA

*alessio.cardillo@urv.cat; naokimas@buffalo.edu

ABSTRACT

The organisation of a network in a maximal set of nodes having at least k neighbours within the set, known as k -core decomposition, has been used for studying various phenomena. It has been shown that nodes in the innermost k -shells play a crucial role in contagion processes, emergence of consensus, and resilience of the system. It is known that the k -core decomposition of many empirical networks cannot be explained by the degree of each node alone, or equivalently, random graph models that preserve the degree of each node (*i.e.*, configuration model). Here we study the k -core decomposition of some empirical networks as well as that of some randomised counterparts, and examine the extent to which the k -shell structure of the networks can be accounted for by the community structure. We find that preserving the community structure in the randomisation process is crucial for generating networks whose k -core decomposition is close to the empirical one. We also highlight the existence, in some networks, of a concentration of the nodes in the innermost k -shells into a small number of communities.

Introduction

Whenever a system can be abstracted as a set of units (*nodes*) interacting in pairs (*edges*), we can describe it as a network (also called a graph). Network analysis has proven to be a valuable framework to aid us to understand a plethora of phenomena taking place in many complex systems. Examples include cascades and collective behaviour in socio-technical systems, the emergence of cognitive functions in neural systems, the stability of chemical/biological systems, and the shape of spatially embedded systems, to cite a few¹⁻³.

One of the advantages of the network representation is the possibility to probe the system in a coarse-grained manner, going beyond dyadic interactions by identifying high-order structures of the network^{4,5}. Examples include tightly connected groups of nodes, *i.e.*, communities⁶, multiscale coarse-grained structures⁷, core-periphery structure⁸⁻¹⁰, nested assembly of nodes¹¹, rich clubs^{12,13}, and the k -core^{14,15}.

The k -core decomposition of a network is the maximal set of nodes that have at least k neighbours within the set^{14,15}. The algorithm to extract the k -core consists in recursively removing the nodes having less than k connections. A k -shell is defined as the set of nodes belonging to the k^{th} core but not to the $(k+1)^{\text{th}}$ core¹⁵. The k -core decomposition has proven to be useful in a variety of domains such as identifying and ranking the most influential spreaders in networks, identifying keywords used for classifying documents, and in assessing the robustness of mutualistic ecosystem and protein networks^{16,17}.

Models to generate random networks with specific features should help us to understand how the mechanisms governing the establishment of edges account for properties of empirical networks. Despite the vast range of applications of the k -core decomposition, to the best of our knowledge, there have been only few attempts to build models to generate networks with a given k -core structure. One indirect attempt to generate networks with a given k -core decomposition is the so-called BRITE model¹⁸. Originally, this model sought to replicate the features (including the k -core) of the Internet network at the Autonomous System (AS) level by mixing the mechanism of growth with preferential attachment^{19,20} and that of adding edges between already existing nodes. Another model aimed at generating networks with a k -core structure akin to an empirical one by leveraging the information stored in the so-called core fingerprint²¹. The core fingerprint corresponds to knowing the number of nodes in each k -shell, the number of intra-shell edges (*i.e.*, those connecting nodes belonging to the same k -shell), and the number of inter-shell edges (*i.e.*, those connecting nodes belonging to different k -shells) of a given network. Moreover,

the authors qualitatively compared the Internet AS networks and synthetic networks preserving the core fingerprint of the original networks using several indicators²¹. More recently, models based on modified versions of the so-called configuration model have been proven to be effective in generating networks with k -core structure akin to that of empirical networks^{22,23}. In a nutshell, in these models the edge stubs attached to each node are divided into two groups: red and blue. Red stubs can create any edges regardless of the k -shell structure. Blue stubs only form edges connecting nodes belonging to distinct k -shells. Among the possible pairs of stubs' colours, only the blue-blue pair is forbidden.

As mentioned above, another type of mesoscale structure is communities. Although there is not a univocal definition of what a community is, in general the community refers to a group of nodes that are more tightly connected between each other than with the other nodes of the network⁶. Communities are also defined by the concept of stochastic equivalence, *i.e.*, nodes in the same group/community interact, on average, with nodes in other groups in the same way²⁴. Methods based on different definitions of communities may return different partitions of the node set. However, there is often some consistency between those partitions, which indicates the presence of groups of nodes acting like the building blocks of communities²⁵. The presence of communities is an important large-scale characteristic of many empirical networks because a system's different functions tend to be located in different communities (*e.g.*, in functional brain networks²⁶ and protein-protein interaction networks²⁷). Moreover, it has been proven that communities play a role in the resilience of the system²⁸ and the presence of triangles²⁹, as well as in the emergence of collective behaviour including synchronisation³⁰, the emergence of cooperation^{31,32}, spreading of a pandemic³³, and the attainment of consensus^{34,35}.

Although k -core and communities are two ways of decomposing the same network, there may be overlaps or intricate relationships between them. In the present paper, we study the relation between the k -core decomposition and the community structures of several empirical and synthetic networks. In particular, we leverage the work of Alvarez-Hamelin *et al.*³⁶ and confirm that the nodes' degrees (*i.e.*, their number of edges) alone are not capable of reproducing the network's k -shell structure. We find that one has to include information about the community structure to obtain networks whose k -core decomposition looks sufficiently close to the empirical one. We also highlight the existence of a concentration-like phenomenon of the innermost k -shells into a small number of communities, which is stronger in some data sets than others.

Results

Degree-based reconstruction of the k -core

As stated above, various studies on networks leverage the k -core decomposition to extract insightful information from networks. However, less studies have asked which mechanisms are sufficient for explaining generation of networks having empirically observed patterns of k -core decomposition. More specifically, Alvarez-Hamelin *et al.* found that networks generated using the configuration model³⁷ having a Poisson or power-law distribution do not display a k -core structure similar to the one displayed by the AS network³⁶. Using the results of Alvarez-Hamelin *et al.* as a starting point, given an empirical network G with N nodes, we check whether its k -core decomposition can be reproduced solely from the degree of each node i (*i.e.*, the number of edges that node i has), denoted by k_i . We generated random networks by a standard configuration model preserving the degree of each node of G , which we denote by deg (see Methods for details).

We have analysed several empirical networks encompassing social, technological, linguistic, and transportation systems whose main properties are summarised in Table 1. In Fig. 1, we show the survival function of the probability distributions of the k -shell index, $P_{\geq}(k_s)$ (*i.e.*, fraction of nodes whose k -shell index is larger than or equal to k_s), for a selection of data sets, compared across the original networks and their synthetic counterparts (see Supplementary Fig. S1 in SM for the other data sets). Figure 1 indicates that the degree of each node is not sufficient for reproducing the k -core structure of the original networks because $P_{\geq}(k_s)$ for deg considerably deviates from that for the original networks. This result is consistent with the previous results³⁶. In fact, we find that fixing the degree of each node is sufficient to recover the k -core profile in some networks. For these networks the empirical and deg networks are not too different in terms of $P_{\geq}(k_s)$ (*e.g.*, Facebook 2 and Cookpad networks). We point out two main differences in $P_{\geq}(k_s)$ between the empirical and deg networks. First, for most data sets, the largest k_s value, which is denoted by D and called the degeneracy, is considerably smaller for the networks generated by deg than the original networks. Second, the $P_{\geq}(k_s)$ of some empirical networks have plateaus and abrupt drops in $k_s \leq D$. The plateaus imply that some of the k -shells are completely or almost empty, whereas the abrupt drops indicate that some k -shells are more densely populated than those adjacent to them. In contrast, $P_{\geq}(k_s)$ for the deg networks does not have a notable plateau or drop in $k_s \leq D$. Therefore, in the deg networks, all the k -shells up to $k_s = D$ are populated, and there is no k -shell that is substantially more populated than its adjacent k -shells.

A more quantitative comparison of distribution $P_{\geq}(k_s)$ between the empirical and deg networks may be done by, for example, the Kolmogorov-Smirnov (KS) test³⁸. However, because a majority of the nodes usually belongs to outer k -shells, (*i.e.*, set of nodes with small k_s values) and Fig. 1 shows that the strongest discrepancies between the two distributions tend to occur at large k_s values, the KS test fails to grasp the differences at large k_s values that we are mostly interested in. Therefore, we compare the k -core decomposition of the empirical and deg networks using four indicators, *i.e.*, the relative

difference in the average k -shell index, $\Delta\langle k_s \rangle$, the relative difference in the network's degeneracy, ΔD , the Jaccard score, J , and Kendall's, τ_K of the nodes belonging to the top 10% (*i.e.*, innermost k -shells) of the $P_{\geq}(k_s)$ distribution. The average of each indicator over all the data sets for the networks obtained with the `deg` shuffling method is equal to $\langle \Delta\langle k_s \rangle \rangle = 0.052 \pm 0.056$, $\langle \Delta D \rangle = 0.302 \pm 0.288$, $\langle J \rangle = 0.563 \pm 0.194$, and $\langle \tau_K \rangle = 0.763 \pm 0.176$. The value of $\langle \Delta\langle k_s \rangle \rangle$ indicates that $\langle k_s \rangle$ is only $\approx 5\%$ different between the original and `deg` networks on average. However, their degeneracy differs by $\approx 30\%$ on average. The $\langle J \rangle$ and $\langle \tau_K \rangle$ values inform us that innermost k -shells of the original networks and those of the `deg` networks tend to share approximately half of the nodes, albeit their ranking seems to be fairly preserved. The values of each indicator are reported in Supplementary Table S1.

Community-aware reconstruction of the k -core

We have seen that the degree distribution by itself does not reproduce main features of the k -shell index distribution. An alternative feature that may explain the k -shell index distribution is the community structure. For this reason, we generated synthetic networks that preserve both the degree of each node and the community structure, $\mathcal{C} = \{C_1, \dots, C_{N_c}\}$, where N_c is the number of communities of the original network. To account for the multiple definitions of what a community is, we identified the communities of each network using two methods: the Louvain method³⁹, denoted by `Lvn`, and the degree-corrected stochastic block model⁴⁰, denoted by `SBM`. In combination with each of the two community detection methods, we considered two rewiring methods preserving \mathcal{C} and the degree of each node, denoted by `commA` and `commB`. Method `commA` preserves the exact number of inter- and intra-community edges at the level of single communities. Method `commB` preserves the number of inter- and intra-community edges for each node.

Figure 1 indicates that preserving the community structure in addition to the degree of each node improves the similarity in $P_{\geq}(k_s)$ between the empirical and synthetic networks, especially at large k_s values, which correspond to inner k -shells. In particular, `commA` and `commB` generate networks whose D value tends to be closer to the empirical value than `deg` does. Furthermore, $P_{\geq}(k_s)$ for `commA` and `commB` tends to have plateaus and abrupt drops at $k_s \leq D$ similarly to the empirical networks. Overall, synthetic networks preserving the `SBM` community structure have a k -core decomposition more akin to the empirical one than those preserving the `Lvn` community structure. This observation is quantitatively supported by the values of the four indices reported in Supplementary Table S1.

To obtain an overview of the performances of different network randomisation methods, in Fig. 2 we show the fraction of data sets, f_X , for which a certain shuffling method generates a k -core decomposition that is the most similar to that of the empirical network according to each indicator. The figure indicates that `commB-SBM` (*i.e.*, the `commB` shuffling method that preserves the community structure determined by `SBM`) performs the best in mimicking the k -shell index features for approximately 65%–80% of the data sets, depending on the indicator. Detailed results for the performance of each method for each empirical network are shown in Supplementary Fig. S2 and Supplementary Table S1.

One issue of `Lvn` is that it cannot discover small communities^{6,41}. One way to mitigate this limitation is to introduce in `Lvn` a resolution parameter, $r \in (0, 1]$, regulating the resolution scale. It is possible to detect small communities when r is small, whereas the original `Lvn` corresponds to $r = 1$ ⁴². We denote by `LvnR` the Louvain method with $r < 1$, *i.e.*, with a resolution higher than that used by `Lvn`. In Sec. 2 of SM we report whether preserving the communities found using `LvnR` instead of `Lvn` improves our ability to reproduce the k -core decomposition of the original network. We found that `LvnR` performs better than `Lvn` (Supplementary Figs. S3 and S4) but worse than `SBM` in general (Supplementary Fig. S5).

Imposing the simultaneous conservation of each node's degree and community structure may result in synthetic networks that are not substantially different from the original ones. To exclude this possibility, we computed the Jaccard score, $J(\mathcal{L}, \mathcal{L}')$, (see Eq. (3)) for the sets of edges, \mathcal{L} and \mathcal{L}' , of the original and shuffled networks, respectively. The values of J approximately fall between 0.01 and 0.5, confirming that the set of edges – hence, the networks – are considerably different.

The results presented so far suggest that preserving the community structure improves the preservation of the k -core decomposition of the original network. Therefore, the mere presence of a community structure may be enough to preserve the main features of the k -core decomposition of the original networks. To test this possibility, we applied the k -core decomposition to networks with communities generated using the LFR model⁴³ (see Sec. 3 of SM). The plots of $P_{\geq}(k_s)$ shown in Supplementary Figs. S7–S10 indicate that the presence of a community structure alone is not sufficient for producing major features of the k -core structure of the empirical networks. Specifically, the $P_{\geq}(k_s)$ of the networks generated by the LFR model is always smooth and shows neither plateaus nor abrupt drops as k_s increases. Moreover, with the LFR, k_s is narrowly distributed, *i.e.*, $\max(k_s) - \min(k_s) \approx 10$. These differences between the k -core structure of the LFR model and that of empirical networks are not sensitive to the value of the mixing parameter, μ , of the LFR model, which controls how distinct the communities are. It should also be noted that for the LFR model, as for the empirical network, the `commB-SBM` generates networks that are the most similar to the original LFR networks among the different shuffling methods in terms of $P_{\geq}(k_s)$.

Overlap between communities and k -core

Preserving the community structure in addition to the node's degree can lead to preservation of features of the k -core structure possibly because nodes with high values of k_s form a k -core which tend to belong to the same community. To examine this possibility, we show the number of communities to which the nodes of a given k -shell belong, $n_C(k_s)$, in Fig. 3 (see Supplementary Fig. S11 for the other data sets). Although each data set shows a distinct pattern, for many data sets, inner k -shells (*i.e.*, nodes with large k_s values) are concentrated into one or a few communities. The concentration effect is particularly noticeable for some data sets, *e.g.*, Facebook 1 and Twitter. To check whether the number of communities per k -shell is merely a byproduct of the random combinatorial effect owing to the number of communities, the distribution of the community size, and the distribution of k_s , we computed a random assignments of the nodes to communities and then calculated $n_C(k_s)$ for each k_s value (see Sec. 4 and Supplementary Fig. S12 of the SM). We have found that the nodes in each k -shell are almost always more concentrated into a smaller number of communities than what is expected by the random assignment of the nodes to communities for all the data sets and community detection methods, with the only exception of SBM for Cookpad's data sets. This finding is in agreement with the previous result that nodes with high k_s tend to belong to the same community, which has been observed in networks embedded into hyperbolic spaces^{44,45}. In particular, we observe a strong concentration of the k -shells into a few communities for the Facebook 1, Twitter, Cond. Matter, Comp. Science, and Words networks, which are those showing a more pronounced difference in the values of D between the original and deg networks.

Discussion

The information encoded in the degree of each node is not sufficient for generating networks with a k -core structure that is similar to those of empirical networks³⁶. This gap of knowledge calls for the design of generative models of networks beyond the configuration model. Such models are expected to be useful to generate benchmark networks and to understand the mechanisms behind the emergence of the k -core. To the best of our knowledge, few models are available to generate networks with a given k -core decomposition^{21–23}.

In the present study, we investigated how much the combination of the nodes' degrees and community structure accounts for k -core structure of empirical networks. Given a network G , we randomly shuffled G 's edges to generate its synthetic counterparts preserving each node's degree and/or community structure of G . We found that randomised networks preserving the community structure obtained through a stochastic block model showed a k -shell index distribution that was reasonably similar to the distribution for the original networks. The success of the stochastic block model in mimicking the features of the k -core decomposition might be due to its ability to approximate the mesoscale structures of networks with a good accuracy^{24,46}, including communities. We also sought to understand more the relationship between k -core and communities by studying networks generated by the LFR model which enables us to control the extent to which the communities are distinguished from each other. However, regardless of whether or not different communities are relatively distinguished from each other in a network, the k -shell index distribution of LFR networks does not show the same features as those observed in the empirical networks. Finally, we have investigated the overlap between communities and k -shells and found that, in some empirical networks, the nodes in inner k -shells are concentrated into a small number of communities much more so than a randomised counterpart. This result is in agreement with the observations made for networks embedded in hyperbolic spaces^{44,45}. Up to our numerical efforts, the concentration is observed if and only if the empirical network and its deg counterpart are substantially different in terms of their k -core decomposition. The concentration suggests that inner k -shells may perform specific functions in such networks, corresponding to the functions of the communities they belong to as observed in, for instance, functional brain networks²⁶ and protein-protein interaction networks²⁷.

The "community aware" rewiring mechanisms introduced in this paper can be used for assessing whether or not a given property of a network is a direct expression of its community structure. One example of such an approach is given in⁴⁷, where the authors have improved the robustness against attacks on a network while keeping its community structure. In that case, the method only preserves the communities and alters the connectivity pattern by increasing the density of intra-community edges as well as changing the edges between communities. It may be interesting, instead, to check whether the robustness of the network can be improved even when one also preserves the degree of the nodes using our community-aware rewiring mechanisms.

One viable extension of our work is to the case of k -peak graph decomposition method⁴⁸. In Ref.⁴⁸, the authors argue that for networks with communities, the k -core decomposition should be performed locally rather than globally, thus returning the k -peak decomposition of each of the system's regions. The rationale behind this approach is to avoid that, if the network contains regions with different densities of edges, the standard k -core decomposition would fail to recognise local core nodes in sparser regions. Studying the evolution of the k -peak decomposition in response to the rewiring of the connections may unveil salient features of complex systems. Another possible direction of research is to concatenate the information encoded into the k -shell index, k_s , with the one provided by the so-called onion decomposition (OD)⁴⁹. The OD is an extension of the k -core decomposition where a node is labelled with both its k_s and its layer index. The layer of a node i represents the iteration

number with which node i is removed in the recursive pruning process of the k -core decomposition. The OD provides a further characterisation of the structure of the network than the k -core, revealing, for example, how tree-like the network is.

Summing up, in this work we have analysed the interplay between the k -core decomposition and community structure of networks. Understanding such a relationship is useful not only owing to the broad range of applications of k -core decomposition, but also to inform the design of models capable of generating networks with both a community structure and k -core's features beyond those explainable by the degree distribution. Such models may stand on, for instance, the stochastic block model⁴⁰, the enhanced configuration model based on maximum entropy⁵⁰, or the hierarchical extension of the LFR model⁵¹. Alternatively, models based on microscopic growth mechanisms such as triadic closure^{52,53} or modified preferential attachment⁵⁴ may deserve further investigation.

Methods

Data

We have considered networks corresponding to systems of different types: from social to technological, from semantic to transportation. Table 1 summarises main properties of such networks. Except for Cookpad networks, all the data sets are publicly available and have been retrieved from the Stanford Large Network data set Collection⁵⁵ (Facebook 1, Twitter, Emails, and Cond. Matter), the Network Repository^{56–58} (Facebook 2, 3, 4, and 5), the Koblenz Network Collection (KONECT)⁵⁹ (Comp. Science, and Words), Mark E. J. Newman's personal network data repository⁶⁰ (Web-blogs), and the OpenFlights data repository⁶¹ (Global airline). In the following text, we provide a brief description of each data set.

Facebook & Twitter. These networks describe social relationships. Nodes are people. Edges represent their friendship relations.

Web-blogs. This network is composed of the hyperlinks (edges) between weblogs on US politics (nodes) recorded in 2005.

Emails. This is a network of email data from a large European research institution. Nodes are people. Edges connect pairs of individuals who have exchanged at least one e-mail.

Cond. Matter & Comp. Science. The former network is the co-authorship network of the authors of preprint manuscripts submitted to the Condensed Matter Physics arXiv e-print archive from January 1993 to April 2003. The latter network is similarly defined using manuscripts appearing in the DBLP computer science bibliography, using a comprehensive list of research papers in computer science. The submission time of the papers of the DBLP collection is unavailable. A node is an author. An edge represents the existence of at least one manuscript co-authored by two authors.

Global airline. In this network nodes are airports across the globe. An edge indicates direct commercial flights between two airports.

Words. This network accounts for the lexical relationships among words extracted from the WordNet data set. Nodes are English words. Edges are relationships (synonymy, antonymy, meronymy, etc.) between pairs of words.

Cookpad. These networks are extracted from the Cookpad online recipe sharing platform⁶². Users can post and browse recipes, as well as interact with other users through recipes in multiple ways including liking, sharing, and posting a comment. The platform is present in many countries (*e.g.*, Japan, Indonesia, United Kingdom, and Italy). Here, we consider the data collected from September to November of 2018 in Greece, Spain, and the United Kingdom, separately for each country. In the three networks, nodes are users. An edge between a pair of users exists if one or more of the following types of events takes place: like or follow a user, viewing, bookmarking, commenting, or making a cooksnap of another user's recipe.

All the networks considered in this work are treated as undirected and unweighted, even when the original data contains more information. Finally, we also consider synthetic networks, generated using the LFR (Lancichinetti–Fortunato–Radicchi) model⁴³ (see Sec. 3 of SM for details).

Network shuffling

Given a network, G , with N nodes and L edges, we generate a randomised counterpart, G' , that has the same nodes and the same number of edges by shuffling the edges of G . We consider three shuffling methods denoted by `deg`, `commA`, and `commB`; each shuffling method preserves different properties of G . The shuffling consists in selecting uniformly at random two edges (a, b) and (c, d) , and replacing them with, *e.g.*, (a, c) and (b, d) , if the swapping of the edges is accepted. An attempt to swap edges is accepted, in which case we call the swapping effective, if and only if it respects the rule of the specific shuffling method and the

swapping does not generate self-loops or multiple edges. We continued the shuffling until we carried out $2L$ effective swaps, such that an edge was swapped four times on average.

In the following text, we provide the details of each shuffling method. Assume that network G partitions into communities such that the set of the communities is $\mathcal{C} = \{C_1, \dots, C_{N_c}\}$, where N_c is the number of communities. Furthermore, let $g(i) \in \mathcal{C}$, $i = 1, \dots, N$, be the community to which the i th node belongs and k_i be the degree of node i . We have:

Degree-preserving shuffling (deg). This method preserves degree k_i of each node i and is equivalent to the configuration model³⁷.

Community-preserving shuffling of type A (commA). On top of the degree of each node, this method preserves the total number of edges within each community and between each pair of communities. In attempts to swap edges, we replace two randomly selected edges (a, b) and (c, d) by (a, c) and (b, d) if and only if an end node of edge (a, b) and an end node of edge (c, d) belong to the same community (*i.e.*, if $g(b) = g(c)$ or $g(a) = g(d)$).

Community-preserving shuffling of type B (commB). Like commA, this method preserves the degree of each node and the number of edges within each community and between each pair of communities. In contrast with commA, the commB method preserves the numbers of edges within and across communities for each node, and not only for each community or pairs of communities. Given two selected edges (a, b) and (c, d) , we replace them with (a, c) and (b, d) if and only if the two new edges connect the same community pairs as before the swapping (*i.e.*, $g(b) = g(c)$ and $g(a) = g(d)$).

Comparison of the k -core decomposition

To assess the similarity between the k -core decomposition of the original network, G , and of its shuffled counterpart, G' , we used four indicators: the average k -shell index, $\langle k_s \rangle$, the network's degeneracy, D , the Jaccard score, J , and the generalised Kendall's tau, τ_K . The indicator $\langle k_s \rangle$ explicitly depends on all the nodes in the network, whereas D , J and τ_K only depend on the nodes belonging to the innermost k -shell(s). We use the latter three indicators because, although a majority of nodes tends to belong to outer k -shells, it is a difference in the tails of the k_s distributions that often affect functions of networks such as the impact of influencers in contagion processes⁶³. The four indicators are defined as follows.

The average of the k -shell index, $\langle k_s \rangle$, is equal to

$$\langle k_s \rangle = \frac{1}{N} \sum_{i=1}^N k_s(i), \quad (1)$$

where $k_s(i)$ is the k -shell index of node i . The degeneracy, D , of a network G is given by⁶⁴

$$D = \max_{i \in G} \{k_s(i)\}. \quad (2)$$

Rather than using these raw indicators, to compare across the different data sets, we compute their relative difference between the empirical network and its shuffled counterpart given by $\Delta X = |X_G - X_{G'}|/X_G$, where $X \in \{\langle k_s \rangle, D\}$.

To compute J and τ_K , we need to define a criterion to select nodes belonging to the innermost k -shells. We decided to confine the comparison to the nodes whose k_s falls within the top 10% among the N nodes. The horizontal lines in Fig. 1 indicate the threshold values of k_s^* such that $P_{\geq}(k_s^*) = 0.1$. In the same manner, we define $k_s^{*'}$ such that $P_{\geq}(k_s^{*'}) = 0.1$ in network G' . To calculate J and τ_K , we use the nodes belonging to k -shells with $k_s \geq k_s^*$ in G and the nodes belonging to k -shells with $k_s \geq k_s^{*'}$ in G' without duplication of the nodes. There are several remarks. First, it may hold that $k_s^* \neq k_s^{*'}$. Second, the value of $k_s^{*'}$ varies from one combination of a run of shuffling and community detection to another. Third, as in the case of the Facebook 2 data set, $k_s^{*'}$ sometimes does not even exist. In such a case, we set $k_s^{*'} = D$ and select all the nodes belonging to the innermost k -shell although they constitute more than 10% of the nodes in the network. Fourth, additional tests using different threshold percentages, 5% and 20%, instead of 10%, did not qualitatively change the results. Fifth, while the Jaccard score simply compares the nodes belonging to two sets, the generalised Kendall's tau, τ_K compares ranked sets. In our case, the node's rank is equivalent to the k_s value.

Given two sets \mathcal{A} and \mathcal{B} , the Jaccard score quantifies their overlap and is given by

$$J(\mathcal{A}, \mathcal{B}) = \frac{|\mathcal{A} \cap \mathcal{B}|}{|\mathcal{A} \cup \mathcal{B}|}. \quad (3)$$

The Jaccard index ranges between 0 and 1. A value of 1 indicates the complete overlap between the two sets (*i.e.*, the sets are the same), whereas a value of 0 indicates that the sets are completely different.

The generalised Kendall's tau, τ_K , measures the consistency between two rankings by assigning penalties to pairs of elements on which the two rankings disagree^{65,66}. Given two sets \mathcal{A} and \mathcal{B} having m_A and m_B elements, respectively, consider

their associated ranking functions \mathcal{X} and \mathcal{Y} . We denote with (z_1, z_2) an arbitrary pair of elements of $\mathcal{A} \cup \mathcal{B}$. We assign a penalty $K_{z_1, z_2}(\mathcal{X}, \mathcal{Y}) = 1$ to (z_1, z_2) if (a) the rankings of the two elements within each set are different (*i.e.*, $\mathcal{X}(z_1) \geq \mathcal{X}(z_2)$ and $\mathcal{Y}(z_1) \leq \mathcal{Y}(z_2)$), (b) the element with the higher rank in one set is missing in the other set, *i.e.*, $\mathcal{X}(z_1) > \mathcal{X}(z_2)$ and $z_1 \notin \mathcal{B}$ (or $\mathcal{X}(z_2) > \mathcal{X}(z_1)$ and $z_2 \notin \mathcal{A}$), or (c) both elements belong to one set each, which is not the same set, *i.e.*, $z_1 \notin \mathcal{B}$ and $z_2 \notin \mathcal{A}$ (and vice-versa). In all the other cases $K_{z_1, z_2}(\mathcal{X}, \mathcal{Y}) = 0$, such that we do not penalise the (z_1, z_2) pair. Finally, we sum the penalties over all the possible pairs of elements and normalise it, thus obtaining the generalised Kendall's tau:

$$\tau_K(\mathcal{X}, \mathcal{Y}) = 1 - \frac{1}{m_A m_B} \sum_{z_1, z_2 \in \mathcal{A} \cup \mathcal{B}} K_{z_1, z_2}(\mathcal{X}, \mathcal{Y}). \quad (4)$$

Index τ_K ranges between 0 and 1. If $\tau_K = 1$, the two rankings are completely coherent. If $\tau_K = 0$, the two sets \mathcal{A} and \mathcal{B} have no pair of elements on which rankings \mathcal{X} and \mathcal{Y} are coherent. The above formulation of the Kendall's tau is the so-called the optimistic approach⁶⁵. This means that we do not penalise the case in which a pairs of elements is present in one set and not in the other set.

Community detection methods

We considered two methods for community detection. The first is the Louvain method (L_{VN})³⁹, which is a heuristic greedy multiscale method that approximately maximises the modularity function. Given a network with N nodes distributed among N_c communities, the modularity, Q , reads

$$Q = \frac{1}{2L} \sum_{i,j=1}^N \left[a_{i,j} - \frac{k_i k_j}{2L} \right] \delta(g(i), g(j)), \quad (5)$$

where $a_{i,j}$ is the element of the network's adjacency matrix A ; $g(i)$ is the community to which the i -th node belongs ($1 \leq g(i) \leq N_c$), and $\delta(g(i), g(j))$ is the Kronecker delta. A large value of Q implies a good partitioning. The Louvain method seeks the partitioning that maximises the modularity. Note that we obtain $Q \approx 0$ for random assignment of nodes to communities and that we obtain $Q \approx 1$ when the network is made of perfectly disjoint communities.

The other community detection method that we used is the stochastic block model⁶⁷. It uses the probabilities $\mathcal{P} = \{p_{C_i, C_j}\}$ with which there exists an edge (a, b) connecting an arbitrarily selected node a in community C_i (*i.e.*, $g(a) = C_i$) and an arbitrarily selected node b in community C_j (*i.e.*, $g(b) = C_j$). Different instances of probabilities \mathcal{P} allow the description of different mixing patterns. When the diagonal entries of \mathcal{P} predominate, we obtain the most usual community structure, whereas other instances yield other structures such as bipartite or core-periphery structure.

To find the optimal partition, one maximises the likelihood function with respect to $\{p_{C_i, C_j}\}$ corresponding to the partitioning $\mathcal{C} = \{C_i\}$, where $i, j \in 1, \dots, N_c$. The unnormalised log-likelihood, \mathfrak{L} , with which a partition of network G into N_c communities, \mathcal{C} , is reproduced reads

$$\mathfrak{L}(G | \mathcal{C}) = \sum_{i,j=1}^{N_c} e_{ij} \log \left(\frac{e_{ij}}{m_i m_j} \right), \quad (6)$$

where e_{ij} is the number of edges connecting community C_i and community C_j , and m_i is the number of nodes belonging to C_i .

The above formulation, however, has one major limitation: it assumes that the degrees of the nodes are distributed according to a Poisson-like function. To account for the degrees' heterogeneity, Karrer *et al.* have implemented the so-called degree corrected stochastic block model, in which the expected degree of each node is kept constant via the introduction of additional parameters⁴⁰. Let e_i be the sum of the node's degree over all nodes in community C_i . Then, the unnormalised log-likelihood for the degree-corrected stochastic block model reads

$$\mathfrak{L}_{DC}(G | \mathcal{C}) = \sum_{i,j=1}^{N_c} e_{ij} \log \left(\frac{e_{ij}}{e_i e_j} \right). \quad (7)$$

Equations (6) and (7) depend on the number of communities N_c . Because the value of N_c is not known a priori, it is inferred through the minimisation of a quantity called the description length. The minimum description length principle describes how much a model compresses the data and allows us to find the optimal number of communities while avoiding overfitting⁶⁸. In the present work we use the degree-corrected stochastic block model and its implementation available in the Python Graph-tool package⁶⁹, which we refer to as SBM for brevity.

References

1. Boccaletti, S., Latora, V., Moreno, Y., Chavez, M. & Hwang, D. Complex networks: Structure and dynamics. *Phys. Reports* **424**, 175–308, DOI: [10.1016/j.physrep.2005.10.009](https://doi.org/10.1016/j.physrep.2005.10.009) (2006).
2. Barabási, A.-L. The network takeover. *Nat. Phys.* **8**, 14–16, DOI: [10.1038/nphys2188](https://doi.org/10.1038/nphys2188) (2011).
3. Vespignani, A. Modelling dynamical processes in complex socio-technical systems. *Nat. Phys.* **8**, 32–39, DOI: [10.1038/nphys2160](https://doi.org/10.1038/nphys2160) (2012).
4. Lambiotte, R., Rosvall, M. & Scholtes, I. From networks to optimal higher-order models of complex systems. *Nat. Phys.* **15**, 313–320, DOI: [10.1038/s41567-019-0459-y](https://doi.org/10.1038/s41567-019-0459-y) (2019).
5. Benson, A. R., Gleich, D. F. & Leskovec, J. Higher-order organization of complex networks. *Science* **353**, 163–166, DOI: [10.1126/science.aad9029](https://doi.org/10.1126/science.aad9029) (2016).
6. Fortunato, S. & Hric, D. Community detection in networks: A user guide. *Phys. Reports* **659**, 1–44, DOI: [10.1016/j.physrep.2016.09.002](https://doi.org/10.1016/j.physrep.2016.09.002) (2016).
7. Gfeller, D. & De Los Rios, P. Spectral Coarse Graining of Complex Networks. *Phys. Rev. Lett.* **99**, 038701, DOI: [10.1103/PhysRevLett.99.038701](https://doi.org/10.1103/PhysRevLett.99.038701) (2007).
8. Borgatti, S. P. & Everett, M. G. Models of core/periphery structures. *Soc. Networks* **21**, 375–395, DOI: [10.1016/S0378-8733\(99\)00019-2](https://doi.org/10.1016/S0378-8733(99)00019-2) (2000).
9. Csermely, P., London, A., Wu, L.-Y. & Uzzi, B. Structure and dynamics of core/periphery networks. *J. Complex Networks* **1**, 93–123, DOI: [10.1093/comnet/cnt016](https://doi.org/10.1093/comnet/cnt016) (2013).
10. Rombach, P., Porter, M. A., Fowler, J. H. & Mucha, P. J. Core-periphery structure in networks (revisited). *SIAM Rev.* **59**, 619–646, DOI: [10.1137/17M1130046](https://doi.org/10.1137/17M1130046) (2017).
11. Mariani, M. S., Ren, Z.-M., Bascompte, J. & Tessone, C. J. Nestedness in complex networks: Observation, emergence, and implications. *Phys. Reports* **813**, 1–90, DOI: <https://doi.org/10.1016/j.physrep.2019.04.001> (2019).
12. Zhou, S. & Mondragon, R. J. The rich-club phenomenon in the Internet topology. *IEEE Commun. Lett.* **8**, 180–182, DOI: [10.1109/LCOMM.2004.823426](https://doi.org/10.1109/LCOMM.2004.823426) (2004).
13. Colizza, V., Flammini, A., Serrano, M. Á. & Vespignani, A. Detecting rich-club ordering in complex networks. *Nat. Phys.* **2**, 110–115, DOI: [10.1038/nphys209](https://doi.org/10.1038/nphys209) (2006).
14. Erdős, P. & Hajnal, A. On chromatic number of graphs and set-systems. *Acta Math. Acad. Sci. Hungarica* **17**, 61–99, DOI: [10.1007/BF02020444](https://doi.org/10.1007/BF02020444) (1966).
15. Seidman, S. B. Network structure and minimum degree. *Soc. networks* **5**, 269–287, DOI: [0378-8733\(83\)90028-X](https://doi.org/10.1016/0378-8733(83)90028-X) (1983).
16. Kong, Y.-X., Shi, G.-Y., Wu, R.-J. & Zhang, Y.-C. k -core: Theories and applications. *Phys. Reports* **832**, 1–32, DOI: [10.1016/j.physrep.2019.10.004](https://doi.org/10.1016/j.physrep.2019.10.004) (2019).
17. Malliaros, F. D., Giatsidis, C., Papadopoulos, A. N. & Vazirgiannis, M. The core decomposition of networks: theory, algorithms and applications. *The VLDB J.* **29**, 61–92, DOI: [10.1007/s00778-019-00587-4](https://doi.org/10.1007/s00778-019-00587-4) (2020).
18. Medina, A., Lakhina, A., Matta, I. & Byers, J. Brite: an approach to universal topology generation. In *MASCOTS 2001, Proceedings Ninth International Symposium on Modeling, Analysis and Simulation of Computer and Telecommunication Systems*, 346–353, DOI: [10.1109/MASCOT.2001.948886](https://doi.org/10.1109/MASCOT.2001.948886) (2001).
19. de Solla Price, D. J. Networks of Scientific Papers. *Science* **149**, 510–515, DOI: [10.1126/science.149.3683.510](https://doi.org/10.1126/science.149.3683.510) (1965).
20. Barabási, A. & Albert, R. Emergence of Scaling in Random Networks. *Science* **286**, 509–512, DOI: [10.1126/science.286.5439.509](https://doi.org/10.1126/science.286.5439.509) (1999).
21. Baur, M., Gaertler, M., Görke, R., Krug, M. & Wagner, D. Augmenting k -core generation with preferential attachment. *Networks & Heterog. Media* **3**, 277–294, DOI: [10.3934/nhm.2008.3.277](https://doi.org/10.3934/nhm.2008.3.277) (2008).
22. Hébert-Dufresne, L., Allard, A., Young, J.-G. & Dubé, L. J. Percolation on random networks with arbitrary k -core structure. *Phys. Rev. E* **88**, 062820, DOI: [10.1103/PhysRevE.88.062820](https://doi.org/10.1103/PhysRevE.88.062820) (2013).
23. Allard, A. & Hébert-Dufresne, L. Percolation and the effective structure of complex networks. *Phys. Rev. X* **9**, 011023, DOI: [10.1103/PhysRevX.9.011023](https://doi.org/10.1103/PhysRevX.9.011023) (2019).
24. Young, J.-G., St-Onge, G., Desrosiers, P. & Dubé, L. J. Universality of the stochastic block model. *Phys. Rev. E* **98**, 032309, DOI: [10.1103/PhysRevE.98.032309](https://doi.org/10.1103/PhysRevE.98.032309) (2018).

25. Riolo, M. A. & Newman, M. E. J. Consistency of community structure in complex networks. *Phys. Rev. E* **101**, 052306, DOI: [10.1103/PhysRevE.101.052306](https://doi.org/10.1103/PhysRevE.101.052306) (2020).
26. Meunier, D., Lambiotte, R. & Bullmore, E. T. Modular and hierarchically modular organization of brain networks. *Front. neuroscience* **4**, 200, DOI: [10.3389/fnins.2010.00200](https://doi.org/10.3389/fnins.2010.00200) (2010).
27. Huttlin, E. *et al.* Architecture of the human interactome defines protein communities and disease networks. *Nature* **545**, 505–509, DOI: [10.1038/nature22366](https://doi.org/10.1038/nature22366) (2017).
28. Gilarranz, L. J., Rayfield, B., Liñán-Cembrano, G., Bascompte, J. & Gonzalez, A. Effects of network modularity on the spread of perturbation impact in experimental metapopulations. *Science* **357**, 199–201, DOI: [10.1126/science.aal4122](https://doi.org/10.1126/science.aal4122) (2017).
29. Orman, K., Labatut, V. & Cherifi, H. *Complex Networks*, vol. 424 of *Studies in Computational Intelligence*, chap. An empirical study of the relation between community structure and transitivity, 99–110 (Springer, Berlin, Heidelberg, 2013).
30. Lotfi, N., Rodrigues, F. A. & Darooneh, A. H. The role of community structure on the nature of explosive synchronization. *Chaos* **28**, 033102, DOI: [10.1063/1.5005616](https://doi.org/10.1063/1.5005616) (2018).
31. Fotouhi, B., Momeni, N., Allen, B. & Nowak, M. A. Evolution of cooperation on large networks with community structure. *J. The Royal Soc. Interface* **16**, 20180677, DOI: [10.1098/rsif.2018.0677](https://doi.org/10.1098/rsif.2018.0677) (2019).
32. Giatsidis, C., Thilikos, D. M. & Vazirgiannis, M. Evaluating cooperation in communities with the k-core structure. In *2011 International conference on advances in social networks analysis and mining*, 87–93, DOI: [10.1109/ASONAM.2011.65](https://doi.org/10.1109/ASONAM.2011.65) (IEEE, 2011).
33. Salathé, M. & Jones, J. H. Dynamics and control of diseases in networks with community structure. *PLOS Comput. Biol.* **6**, 1–11, DOI: [10.1371/journal.pcbi.1000736](https://doi.org/10.1371/journal.pcbi.1000736) (2010).
34. Mistry, D., Zhang, Q., Perra, N. & Baronchelli, A. Committed activists and the reshaping of status-quo social consensus. *Phys. Rev. E* **92**, 042805, DOI: [10.1103/PhysRevE.92.042805](https://doi.org/10.1103/PhysRevE.92.042805) (2015).
35. Masuda, N. Voter model on the two-clique graph. *Phys. Rev. E* **90**, 012802, DOI: [10.1103/PhysRevE.90.012802](https://doi.org/10.1103/PhysRevE.90.012802) (2014).
36. Alvarez-Hamelin, J. I., Dall’Asta, L., Barrat, A. & Vespignani, A. K-core decomposition of internet graphs: hierarchies, self-similarity and measurement biases. *Networks & Heterog. Media* **3**, 371, DOI: [10.3934/nhm.2008.3.371](https://doi.org/10.3934/nhm.2008.3.371) (2008).
37. Fosdick, B. K., Larremore, D. B., Nishimura, J. & Ugander, J. Configuring random graph models with fixed degree sequences. *SIAM Rev.* **60**, 315–355, DOI: [10.1137/16M1087175](https://doi.org/10.1137/16M1087175) (2018).
38. Massey Jr, F. J. The Kolmogorov-Smirnov test for goodness of fit. *J. Am. statistical Assoc.* **46**, 68–78 (1951).
39. Blondel, V. D., Guillaume, J.-L., Lambiotte, R. & Lefebvre, E. Fast unfolding of communities in large networks. *J. Stat. Mech. Theory Exp.* **2008**, P10008, DOI: [10.1088/1742-5468/2008/10/P10008](https://doi.org/10.1088/1742-5468/2008/10/P10008) (2008).
40. Karrer, B. & Newman, M. E. J. Stochastic blockmodels and community structure in networks. *Phys. Rev. E* **83**, 016107, DOI: [10.1103/PhysRevE.83.016107](https://doi.org/10.1103/PhysRevE.83.016107) (2011).
41. Fortunato, S. & Barthélemy, M. Resolution limit in community detection. *Proc. Natl. Acad. Sci. United States Am.* **104**, 36–41, DOI: [10.1073/pnas.0605965104](https://doi.org/10.1073/pnas.0605965104) (2007).
42. Lambiotte, R., Delvenne, J. C. & Barahona, M. Random walks, Markov processes and the multiscale modular organization of complex networks. *IEEE Transactions on Netw. Sci. Eng.* **1**, 76–90, DOI: [10.1109/TNSE.2015.2391998](https://doi.org/10.1109/TNSE.2015.2391998) (2014).
43. Lancichinetti, A., Fortunato, S. & Radicchi, F. Benchmark graphs for testing community detection algorithms. *Phys. Rev. E* **78**, 046110, DOI: [10.1103/PhysRevE.78.046110](https://doi.org/10.1103/PhysRevE.78.046110) (2008).
44. Fagqeh, A., Osat, S. & Radicchi, F. Characterizing the analogy between hyperbolic embedding and community structure of complex networks. *Phys. Rev. Lett.* **121**, 098301, DOI: [10.1103/PhysRevLett.121.098301](https://doi.org/10.1103/PhysRevLett.121.098301) (2018).
45. Osat, S., Radicchi, F. & Papadopoulos, F. k-core structure of real multiplex networks. *Phys. Rev. Res.* 023176, DOI: [10.1103/PhysRevResearch.2.023176](https://doi.org/10.1103/PhysRevResearch.2.023176) (2020).
46. Olhede, S. C. & Wolfe, P. J. Network histograms and universality of blockmodel approximation. *Proc. Natl. Acad. Sci. United States Am.* **111**, 14722–14727, DOI: [10.1073/pnas.1400374111](https://doi.org/10.1073/pnas.1400374111) (2014).
47. Mozafari, M. & Khansari, M. Improving the robustness of scale-free networks by maintaining community structure. *J. Complex Networks* **7**, 838–864, DOI: [10.1093/comnet/cnz009](https://doi.org/10.1093/comnet/cnz009) (2019).
48. Govindan, P., Wang, C., Xu, C., Duan, H. & Soundarajan, S. The k-peak decomposition: Mapping the global structure of graphs. In *Proceedings of the 26th International Conference on World Wide Web*, 1441–1450, DOI: [10.1145/3038912.3052635](https://doi.org/10.1145/3038912.3052635) (International World Wide Web Conferences Steering Committee, 2017).

49. Hébert-Dufresne, L., Grochow, J. A. & Allard, A. Multi-scale structure and topological anomaly detection via a new network statistic: The onion decomposition. *Sci. Reports* **6**, 31708, DOI: [10.1038/srep31708](https://doi.org/10.1038/srep31708) (2016).
50. Mastrandrea, R., Squartini, T., Fagiolo, G. & Garlaschelli, D. Enhanced reconstruction of weighted networks from strengths and degrees. *New J. Phys.* **16**, 043022, DOI: [10.1088/1367-2630/16/4/043022](https://doi.org/10.1088/1367-2630/16/4/043022) (2014).
51. Yang, Z., Perotti, J. I. & Tessone, C. J. Hierarchical benchmark graphs for testing community detection algorithms. *Phys. Rev. E* **96**, 052311, DOI: [10.1103/PhysRevE.96.052311](https://doi.org/10.1103/PhysRevE.96.052311) (2017).
52. Kumpula, J. M., Onnela, J.-P., Saramäki, J., Kaski, K. & Kertész, J. Emergence of communities in weighted networks. *Phys. Rev. Lett.* **99**, 228701, DOI: [10.1103/PhysRevLett.99.228701](https://doi.org/10.1103/PhysRevLett.99.228701) (2007).
53. Bianconi, G., Darst, R. K., Iacovacci, J. & Fortunato, S. Triadic closure as a basic generating mechanism of communities in complex networks. *Phys. Rev. E* **90**, 042806, DOI: [10.1103/PhysRevE.90.042806](https://doi.org/10.1103/PhysRevE.90.042806) (2014).
54. Shang, K.-k., Yang, B., Moore, J. M., Ji, Q. & Small, M. Growing networks with communities: A distributive link model. *Chaos: An Interdiscip. J. Nonlinear Sci.* **30**, 041101, DOI: [10.1063/5.0007422](https://doi.org/10.1063/5.0007422) (2020).
55. McAuley, J. & Leskovec, J. Learning to discover social circles in ego networks. In *Proceedings of the 25th International Conference on Neural Information Processing Systems - Volume 1*, NIPS'12, 539–547 (Curran Associates Inc., Red Hook, NY, USA, 2012).
56. Rossi, R. A. & Ahmed, N. K. The network data repository with interactive graph analytics and visualization. In *Proceedings of the Twenty-Ninth AAAI Conference on Artificial Intelligence*, AAAI'15, 4292–4293 (AAAI Press, 2015).
57. Traud, A. L., Mucha, P. J. & Porter, M. A. Social structure of Facebook networks. *Phys. A* **391**, 4165–4180, DOI: [10.1016/j.physa.2011.12.021](https://doi.org/10.1016/j.physa.2011.12.021) (2012).
58. Traud, A. L., Kelsic, E. D., Mucha, P. J. & Porter, M. A. Comparing community structure to characteristics in online collegiate social networks. *SIAM Rev.* **53**, 526–543, DOI: [10.1137/080734315](https://doi.org/10.1137/080734315) (2011).
59. Kunegis, J. KONECT – The Koblenz Network Collection. In *Proc. Int. Conf. on World Wide Web Companion*, 1343–1350 (2013).
60. Newman, M. E. J. Network data repository: Political blogs dataset. Available at: <http://www-personal.umich.edu/~mejn/netdata/>. Accessed on 01/10/2019.
61. The OpenFlights database. Available at: <https://openflights.org/data.html>. Accessed on 01/10/2019.
62. Cookpad: Make everyday cooking fun! <https://cookpad.com/>. Accessed on 01/10/2019.
63. Kitsak, M. *et al.* Identification of influential spreaders in complex networks. *Nat. Phys.* **6**, 888–893, DOI: [10.1038/nphys1746](https://doi.org/10.1038/nphys1746) (2010).
64. Bollobás, B. *Modern graph theory*. Graduate Texts in Mathematics 184 (Springer-Verlag New York, 1998).
65. Fagin, R., Kumar, R. & Sivakumar, D. Comparing top k lists. *SIAM J. on discrete mathematics* **17**, 134–160, DOI: [10.1137/S0895480102412856](https://doi.org/10.1137/S0895480102412856) (2003).
66. McCown, F. & Nelson, M. L. Agreeing to disagree: search engines and their public interfaces. In *Proceedings of the 7th ACM/IEEE-CS joint conference on Digital libraries*, 309–318, DOI: [10.1145/1255175.1255237](https://doi.org/10.1145/1255175.1255237) (2007).
67. Holland, P. W., Laskey, K. B. & Leinhardt, S. Stochastic blockmodels: First steps. *Soc. Networks* **5**, 109 – 137, DOI: [https://doi.org/10.1016/0378-8733\(83\)90021-7](https://doi.org/10.1016/0378-8733(83)90021-7) (1983).
68. Peixoto, T. P. Nonparametric bayesian inference of the microcanonical stochastic block model. *Phys. Rev. E* **95**, 012317, DOI: [10.1103/PhysRevE.95.012317](https://doi.org/10.1103/PhysRevE.95.012317) (2017).
69. Peixoto, T. P. The graph-tool python library. *figshare* DOI: [10.6084/m9.figshare.1164194](https://doi.org/10.6084/m9.figshare.1164194) (2014).
70. Oliphant, T. *Guide to NumPy* (Trelgol Publishing, 2006).
71. van der Walt, S., Colbert, S. C. & Varoquaux, G. The numpy array: A structure for efficient numerical computation. *Comput. Sci. Eng.* **13**, 22–30, DOI: [10.1109/MCSE.2011.37](https://doi.org/10.1109/MCSE.2011.37) (2011).
72. Hagberg, A. A., Schult, D. A. & Swart, P. J. Exploring network structure, dynamics, and function using networkx. In Varoquaux, G., Vaught, T. & Millman, J. (eds.) *Proceedings of the 7th Python in Science Conference*, 11 – 15 (Pasadena, CA USA, 2008).
73. Hunter, J. D. Matplotlib: a 2d graphics environment. *Comput. Sci. & Eng.* **9**, 90–95, DOI: <https://doi.org/10.1109/MCSE.2007.55> (2007).

74. Stanford Network Analysis Project (SNAP): "social circles: Facebook" dataset. Available at: <http://snap.stanford.edu/data/ego-Facebook.html>. Accessed on 01/10/2019.
75. Network Repository: "American75" dataset. Available at: <http://networkrepository.com/socfb-American75.php>. Accessed on 01/10/2019.
76. Network Repository: "Amherst41" dataset. Available at: <http://networkrepository.com/socfb-Amherst41.php>. Accessed on 01/10/2019.
77. Network Repository: "Cal65" dataset. Available at: <http://networkrepository.com/socfb-Cal65.php>. Accessed on 01/10/2019.
78. Network Repository: "FSU53" dataset. Available at: <http://networkrepository.com/socfb-FSU53.php>. Accessed on 01/10/2019.
79. Stanford Network Analysis Project (SNAP): "social circles: Twitter" dataset. Available at: <http://snap.stanford.edu/data/ego-Twitter.html>. Accessed on 01/10/2019.
80. Adamic, L. A. & Glance, N. The political blogosphere and the 2004 us election: divided they blog. In *Proceedings of the 3rd international workshop on Link discovery*, 36–43, DOI: [10.1145/1134271.1134277](https://doi.org/10.1145/1134271.1134277) (ACM, 2005).
81. Stanford Network Analysis Project (SNAP): "email-EU-core network" dataset. Available at: <http://snap.stanford.edu/data/email-Eu-core.html>. Accessed on 01/10/2019.
82. Yin, H., Benson, A. R., Leskovec, J. & Gleich, D. F. Local higher-order graph clustering. In *Proceedings of the 23rd ACM SIGKDD International Conference on Knowledge Discovery and Data Mining*, 555–564, DOI: [10.1145/3097983.3098069](https://doi.org/10.1145/3097983.3098069) (ACM, 2017).
83. Leskovec, J., Kleinberg, J. & Faloutsos, C. Graph evolution: Densification and shrinking diameters. *ACM Transactions on Knowl. Discov. from Data (TKDD)* **1**, 2 (2007).
84. Stanford Network Analysis Project (SNAP): "Condensed Matter collaboration network" dataset. Available at: <https://snap.stanford.edu/data/ca-CondMat.html>. Accessed on 01/10/2019.
85. The KONECT Project: DBLP co-authorship network dataset. available at: <http://konect.cc/networks/com-dblp> (2017). Accessed on 01/10/2019.
86. Yang, J. & Leskovec, J. Defining and evaluating network communities based on ground-truth. In *Proc. ACM SIGKDD Workshop on Min. Data Semant.*, 3, DOI: [10.1007/s10115-013-0693-z](https://doi.org/10.1007/s10115-013-0693-z) (2012).
87. The KONECT Project: WordNet network dataset. available at: <http://konect.cc/networks/wordnet-words> (2017). Accessed on 01/10/2019.
88. Fellbaum, C. (ed.) *WordNet: an Electronic Lexical Database* (MIT Press, 1998).

Acknowledgements

The authors thank A. Barrat for helpful comments on a preliminary version of this work. A.C. acknowledges the support of the Spanish Ministerio de Ciencia e Innovacion (MICINN) through Grant IJCI-2017-34300. I.M., A.C., and N.M. acknowledge the support of Cookpad Limited. This work was carried out using the computational facilities of the Advanced Computing Research Centre, University of Bristol – <http://www.bristol.ac.uk/acrc/>. Numerical analysis has been carried out using the NumPy, NetworkX, and Graph-tool Python packages^{69–72}. Graphics have been prepared using the Matplotlib Python package⁷³.

Author contributions statement

I.M. analysed data, designed the experiments, and performed simulations, A.C. analysed the results and designed the experiments. All authors discussed the methods and results, and wrote and reviewed the manuscript.

Additional information

Competing interests The authors declare no competing interests.

Data availability The data sets on CookpadTM analysed in the current study are not publicly available due to exclusive ownership of Cookpad Limited. All the other data sets are available from the corresponding repositories listed in the bibliography.

Data set	N	L	$\langle k \rangle$	k_{\max}	$\langle k_s \rangle$	D	N_c^{Lvn}	Q^{Lvn}	N_c^{SBM}	Q^{SBM}	Ref.
Facebook 1	4039	88234	43.691	1045	26.880	115	16	0.835	62	0.551	55,74
Facebook 2	6386	217662	68.168	930	35.712	56	19	0.419	198	0.158	56–58,75
Facebook 3	2235	90954	81.391	467	44.508	63	8	0.436	87	0.139	56–58,76
Facebook 4	11247	351358	62.480	415	32.413	63	10	0.438	274	0.193	56–58,77
Facebook 5	27737	1034802	74.615	2555	38.681	81	18	0.470	547	0.172	56–58,78
Twitter	81306	1342296	33.018	3383	17.762	96	73	0.808	510	0.511	55,79
Web-blogs	1490	16715	22.436	351	12.154	36	275	0.426	17	0.076	60,80
Emails	1005	16064	31.968	345	17.063	34	26	0.410	33	0.232	81–83
Cond. Matter	23133	93439	8.078	279	4.900	25	619	0.730	203	0.633	83,84
Comp. Science	317080	1049866	6.622	343	4.215	113	209	0.822	676	0.726	59,85,86
Global airline	3376	19179	11.362	248	6.123	31	26	0.665	40	0.311	61
Words	146005	656999	9.000	1008	5.289	31	378	0.759	548	0.583	59,87,88
Cookpad Greece	32235	745178	46.234	8196	23.709	158	40	0.166	76	0.020	–
Cookpad Spain	122158	1749751	28.647	12637	14.547	162	262	0.270	90	0.035	–
Cookpad UK	13758	47525	6.909	1880	3.558	33	199	0.350	8	0.114	–

Table 1. Main properties of the data sets used in the present study. N : number of nodes, L : number of edges, $\langle k \rangle$: average degree, k_{\max} : maximum degree, $\langle k_s \rangle$: average value of the k -shell index, D : maximum value of the k -shell index, N_c^{Lvn} , Q^{Lvn} : number of communities determined by the Louvain method and the corresponding modularity, respectively, N_c^{SBM} , Q^{SBM} : number of communities determined by the SBM and the corresponding modularity, respectively.

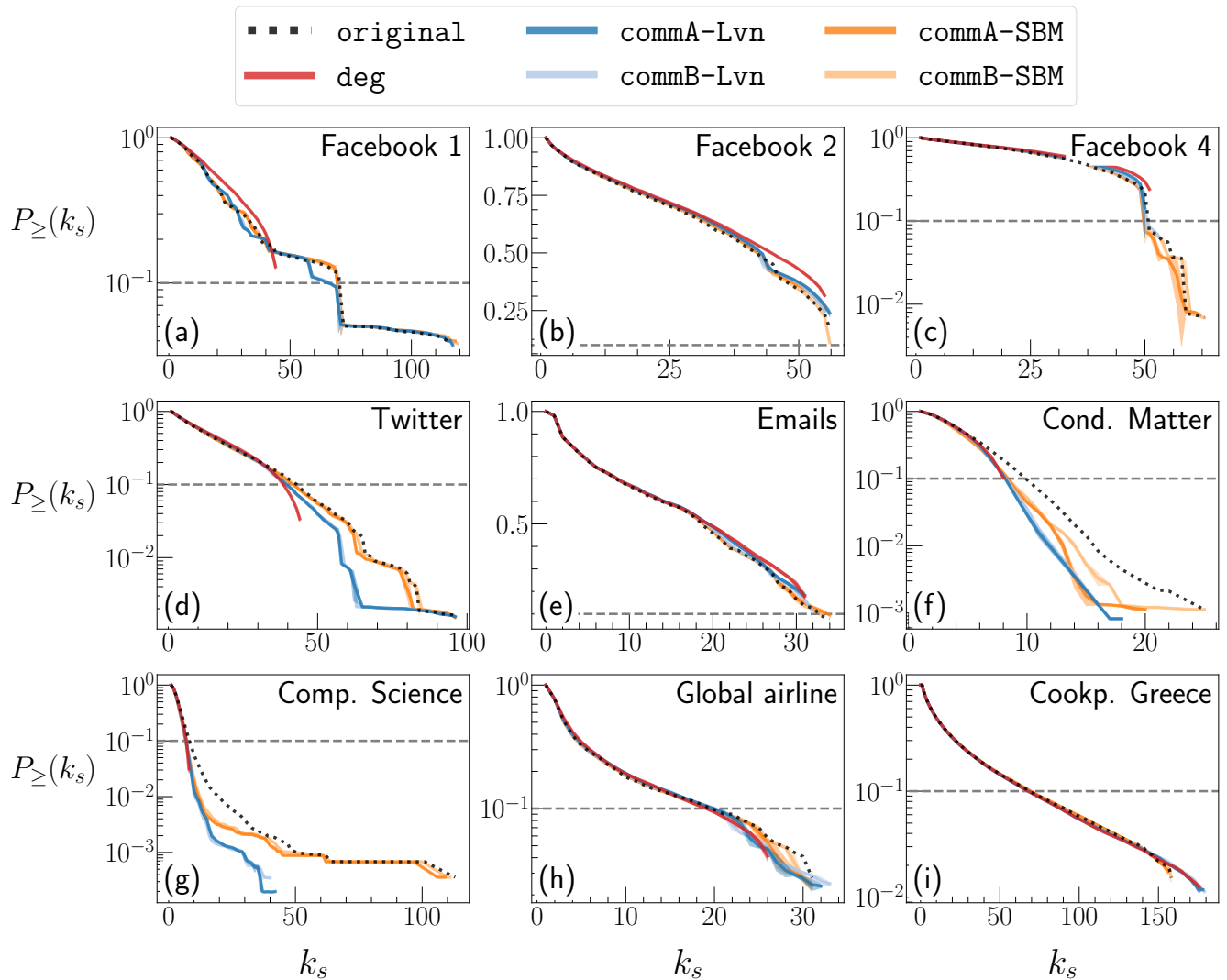


Figure 1. Survival function of the probability distributions of the k -shell index, *i.e.*, $P_{\ge}(k_s)$ as a function of k_s for the original network (dotted line) and shuffled networks (solid line). Each panel corresponds to a data set, *i.e.*, Facebook 1 (panel a), Facebook 2 (b), Facebook 4 (c), Twitter (d), Emails (e), Cond. Matter (f), Comp. Science (g), Global airline (h), and Cookpad Greece (i). The horizontal dashed lines indicate that $P_{\ge}(k_s) = 0.1$. Results are averaged over 10 different runs of each shuffling method, and the shaded areas (when visible) represent the standard deviations.

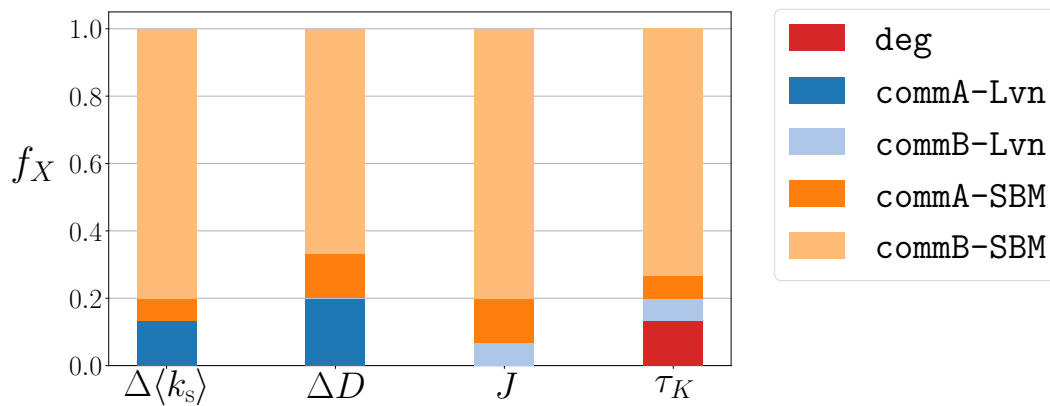


Figure 2. Performances of different shuffling methods in terms of four indicators. We report the fraction of data sets for which a given combination of the shuffling method and the community detection method yields an indicator's value closest to that for the original network. Each bar refers to an indicator, *i.e.*, average k -shell's difference, $\Delta\langle k_s \rangle$, degeneracy's difference, ΔD , Jaccard score, J , and Kendall's tau, τ_K .

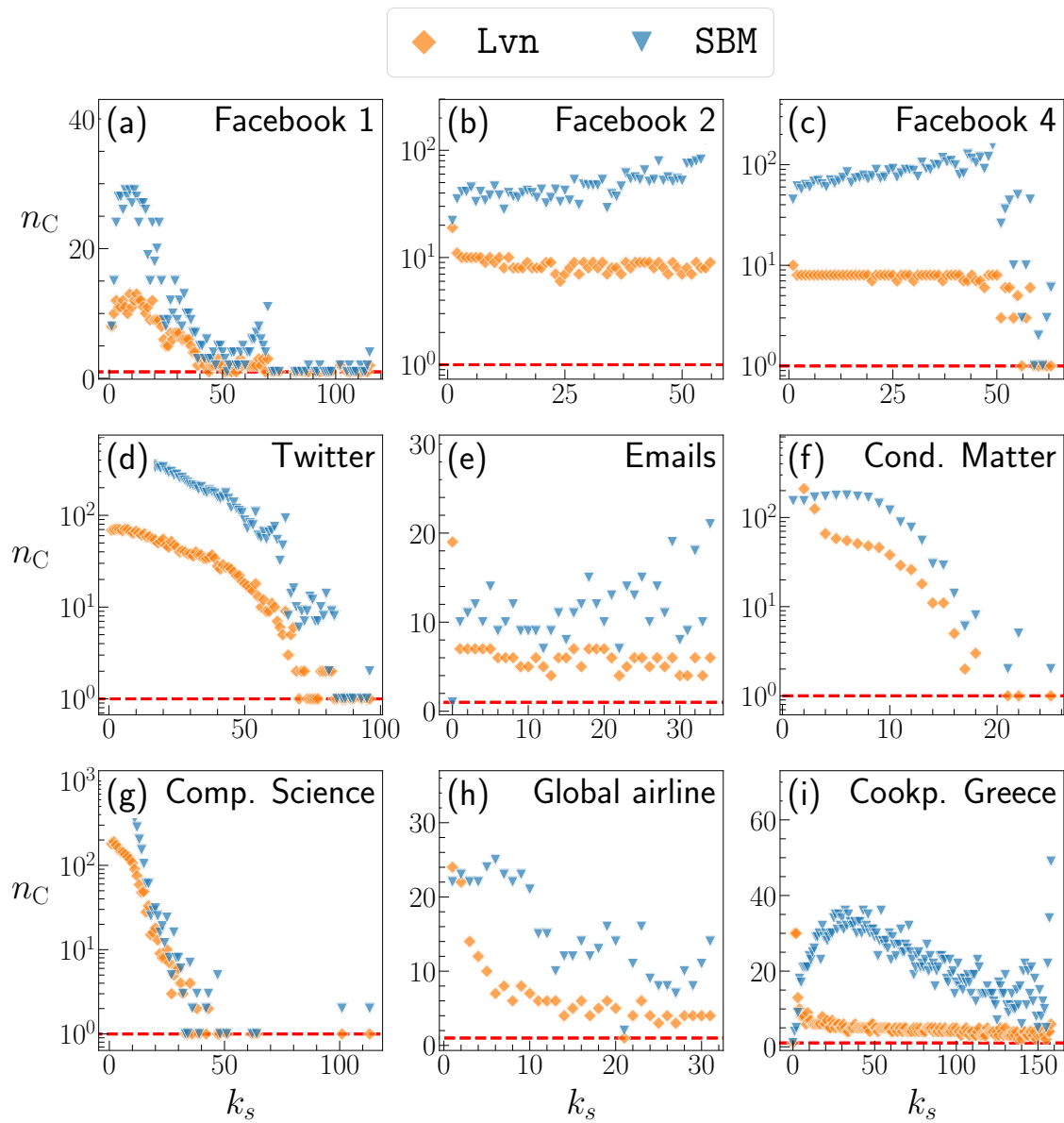


Figure 3. Number of different communities, $n_C(k_s)$, that the set of nodes of a given k -shell value, k_s , overlaps. The horizontal dashed line is a guide to the eyes showing $n_C(k_s) = 1$. Each panel accounts for a different data set (see the caption of Fig. 1 for the details). For each data set, we show the results corresponding to the community structure obtained using either Lvn or SBM.

Supplementary Materials for the manuscript entitled: Interplay between k -core and community structure in complex networks

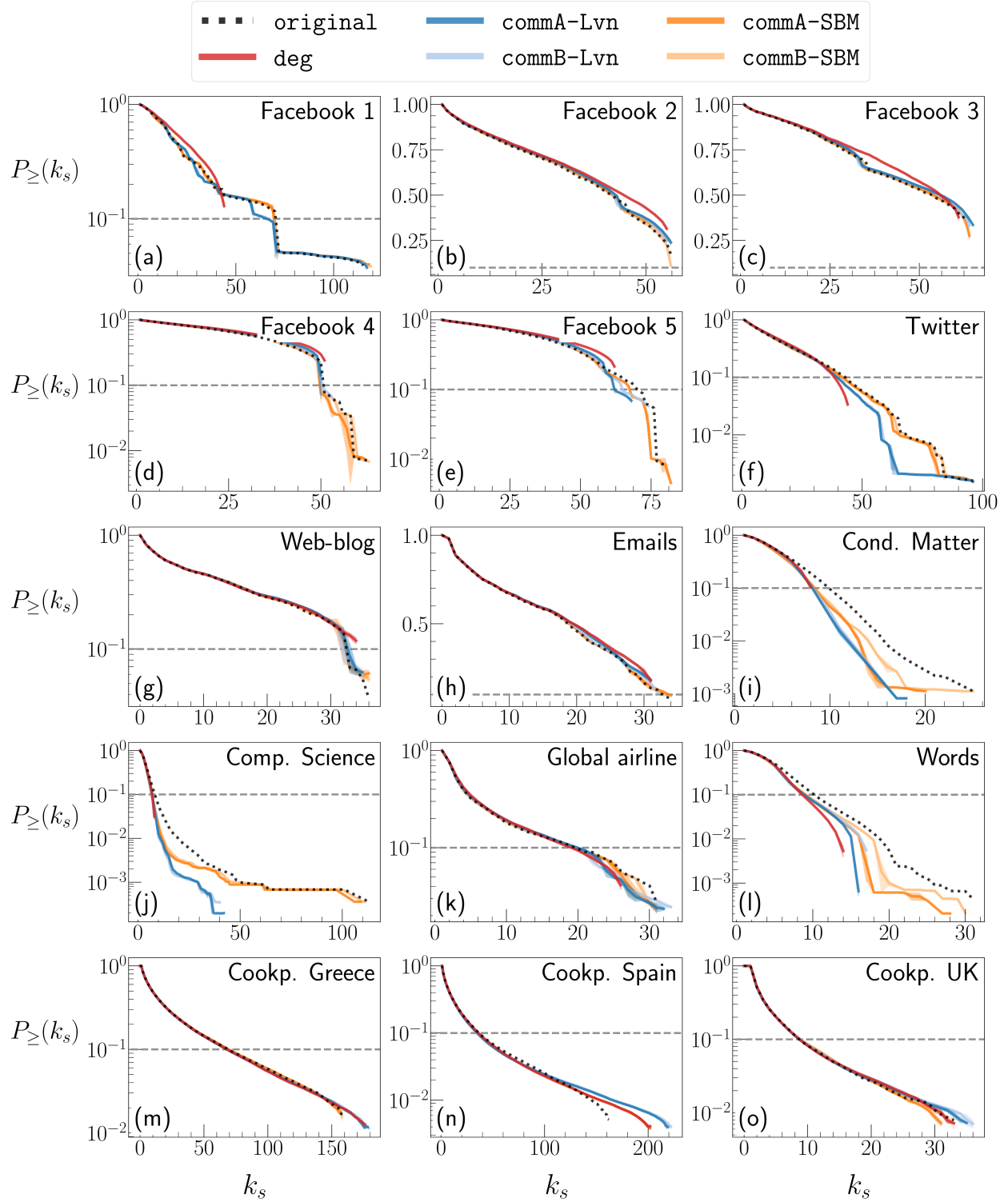
Irene Malvestio, Alessio Cardillo, & Naoki Masuda

1 Comparison between the original and shuffled networks

In this section, we provide a detailed characterisation of the k -core decomposition of the shuffled networks for all the empirical networks. Supplementary Figure S1 shows the survival function of the probability distribution of the k -shell index, $P_{\geq}(k_s)$, of the original networks and their shuffled counterparts (`deg`, `commA`, and `commB`). The figure indicates that `commA` and `commB` produce k -shell distributions that are more similar to the original ones, compared to `deg`, in particular when `commA` or `commB` is combined with SBM. This result also holds true for the Greece and Spain networks of Cookpad where, contrarily to the other data sets, the `deg` networks have a degeneracy, D , higher than the original networks.

In Supplementary Table S1, we report the values of the four indicators used for comparing the k -core decomposition between the original and shuffled networks. In particular, we report the average value and standard deviation of the relative difference $\Delta X = |X(G) - X(G')| / X(G)$ where X is either the average k -shell index, $\langle k_s \rangle$, or D . In the same table, we also report the values of the Jaccard score, J , and Kendall's tau, τ_K , calculated for the set of nodes belonging to the innermost k -shells (see the main text for the details of the methods). We notice that, in general, `commB-SBM` yields the smallest values of $\Delta \langle k_s \rangle$ and ΔD and the largest values of J and τ_K ; confirming its good performances in reconstructing the k -core decomposition of the original network. Supplementary Figure S2 provides an overview of the performances of each shuffling method. Figure 2 in the main text is a projection of the information contained in Supplementary Fig. S2.

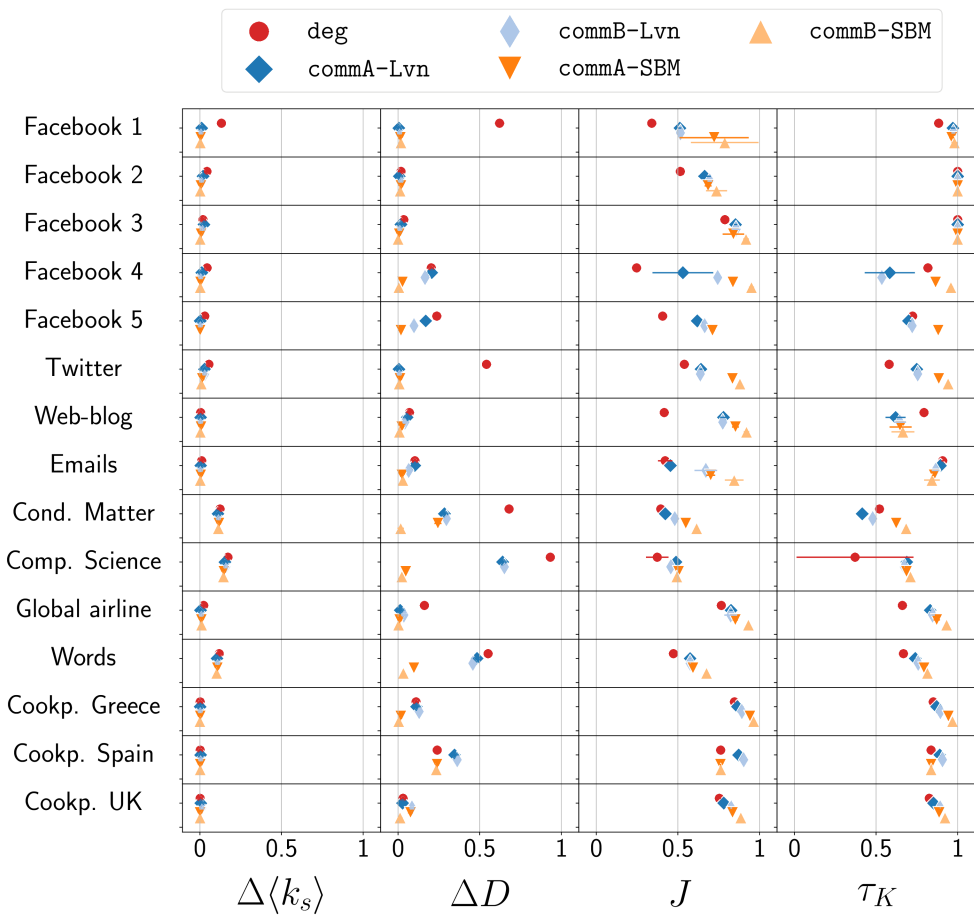
arXiv:2005.01147v3 [physics.soc-ph] 7 Sep 2020



Supplementary Figure S1: Survival function of the probability distribution of the k -shell index, $P_{\ge}(k_s)$, as a function of k_s for the empirical network (dotted lines) and shuffled networks (solid lines). Each panel corresponds to a data set. The horizontal dashed lines represent $P_{\ge}(k_s) = 0.1$. The results shown are averages over 10 different runs of each shuffling method, and the shaded areas (when visible) represent the standard deviations.

Data set	Indicator	deg	commA-Lvn	commB-Lvn	commA-SBM	commB-SBM
Facebook 1	$\Delta \langle k_s \rangle$	0.132 ± 0.002	0.011 ± 0.001	0.007 ± 0.003	0.004 ± 0.002	0.002 ± 0.001
	ΔD	0.622 ± 0.004	0.004 ± 0.006	0.009 ± 0.007	0.014 ± 0.006	0.017 ± 0.007
	J	0.340 ± 0.025	0.512 ± 0.009	0.515 ± 0.004	0.722 ± 0.212	0.787 ± 0.207
	τ_K	0.884 ± 0.005	0.971 ± 0.014	0.974 ± 0.012	0.963 ± 0.015	0.980 ± 0.018
Facebook 2	$\Delta \langle k_s \rangle$	0.043 ± 0.000	0.020 ± 0.003	0.011 ± 0.001	0.006 ± 0.000	0.002 ± 0.001
	ΔD	0.018 ± 0.000	0.007 ± 0.009	0.018 ± 0.000	0.018 ± 0.000	0.012 ± 0.008
	J	0.515 ± 0.008	0.664 ± 0.038	0.695 ± 0.014	0.685 ± 0.021	0.737 ± 0.064
	τ_K	1.000 ± 0.000	1.000 ± 0.000	1.000 ± 0.000	1.000 ± 0.000	1.000 ± 0.000
Facebook 3	$\Delta \langle k_s \rangle$	0.019 ± 0.004	0.025 ± 0.002	0.017 ± 0.003	0.007 ± 0.003	0.002 ± 0.001
	ΔD	0.035 ± 0.006	0.017 ± 0.005	0.011 ± 0.007	0.006 ± 0.008	0.000 ± 0.000
	J	0.788 ± 0.009	0.853 ± 0.009	0.856 ± 0.027	0.840 ± 0.066	0.918 ± 0.017
	τ_K	1.000 ± 0.000	1.000 ± 0.000	1.000 ± 0.000	1.000 ± 0.000	1.000 ± 0.000
Facebook 4	$\Delta \langle k_s \rangle$	0.044 ± 0.003	0.012 ± 0.002	0.005 ± 0.002	0.003 ± 0.001	0.002 ± 0.001
	ΔD	0.203 ± 0.006	0.206 ± 0.000	0.165 ± 0.008	0.027 ± 0.010	0.005 ± 0.007
	J	0.247 ± 0.017	0.531 ± 0.186	0.744 ± 0.015	0.837 ± 0.005	0.951 ± 0.016
	τ_K	0.818 ± 0.011	0.584 ± 0.154	0.535 ± 0.027	0.865 ± 0.008	0.959 ± 0.014
Facebook 5	$\Delta \langle k_s \rangle$	0.030 ± 0.002	0.002 ± 0.001	0.002 ± 0.001	0.001 ± 0.001	—
	ΔD	0.237 ± 0.005	0.169 ± 0.006	0.098 ± 0.004	0.017 ± 0.006	—
	J	0.406 ± 0.023	0.619 ± 0.004	0.664 ± 0.004	0.712 ± 0.015	—
	τ_K	0.724 ± 0.016	0.699 ± 0.016	0.721 ± 0.011	0.881 ± 0.014	—
Twitter	$\Delta \langle k_s \rangle$	0.055 ± 0.000	0.028 ± 0.000	0.030 ± 0.000	0.014 ± 0.000	0.008 ± 0.000
	ΔD	0.542 ± 0.000	0.005 ± 0.005	0.007 ± 0.005	0.011 ± 0.007	0.007 ± 0.005
	J	0.540 ± 0.001	0.641 ± 0.008	0.637 ± 0.005	0.834 ± 0.003	0.881 ± 0.011
	τ_K	0.580 ± 0.004	0.749 ± 0.002	0.755 ± 0.002	0.884 ± 0.002	0.941 ± 0.002
Web-blog	$\Delta \langle k_s \rangle$	0.005 ± 0.002	0.004 ± 0.003	0.004 ± 0.002	0.007 ± 0.004	0.003 ± 0.002
	ΔD	0.069 ± 0.014	0.056 ± 0.012	0.042 ± 0.014	0.022 ± 0.011	0.008 ± 0.013
	J	0.416 ± 0.009	0.780 ± 0.021	0.775 ± 0.022	0.853 ± 0.021	0.920 ± 0.017
	τ_K	0.794 ± 0.018	0.619 ± 0.061	0.646 ± 0.038	0.651 ± 0.068	0.664 ± 0.070
Emails	$\Delta \langle k_s \rangle$	0.011 ± 0.006	0.005 ± 0.002	0.003 ± 0.001	0.005 ± 0.003	0.002 ± 0.001
	ΔD	0.103 ± 0.015	0.103 ± 0.015	0.065 ± 0.012	0.024 ± 0.012	0.029 ± 0.000
	J	0.422 ± 0.044	0.454 ± 0.035	0.671 ± 0.069	0.701 ± 0.027	0.845 ± 0.057
	τ_K	0.908 ± 0.008	0.895 ± 0.008	0.864 ± 0.023	0.855 ± 0.011	0.842 ± 0.048
Cond. Matter	$\Delta \langle k_s \rangle$	0.123 ± 0.001	0.111 ± 0.001	0.113 ± 0.001	0.117 ± 0.001	0.113 ± 0.001
	ΔD	0.680 ± 0.000	0.284 ± 0.012	0.296 ± 0.020	0.244 ± 0.022	0.016 ± 0.020
	J	0.395 ± 0.006	0.423 ± 0.013	0.481 ± 0.008	0.548 ± 0.013	0.615 ± 0.005
	τ_K	0.521 ± 0.018	0.415 ± 0.025	0.479 ± 0.016	0.623 ± 0.013	0.685 ± 0.008
Comp. Science	$\Delta \langle k_s \rangle$	0.171 ± 0.004	0.153 ± 0.000	0.159 ± 0.000	0.146 ± 0.000	0.144 ± 0.000
	ΔD	0.933 ± 0.004	0.641 ± 0.006	0.651 ± 0.004	0.047 ± 0.007	0.023 ± 0.004
	J	0.374 ± 0.069	0.488 ± 0.002	0.456 ± 0.002	0.504 ± 0.003	0.493 ± 0.002
	τ_K	0.371 ± 0.358	0.688 ± 0.003	0.673 ± 0.002	0.686 ± 0.002	0.711 ± 0.002
Global airline	$\Delta \langle k_s \rangle$	0.023 ± 0.001	0.004 ± 0.003	0.008 ± 0.003	0.009 ± 0.003	0.010 ± 0.002
	ΔD	0.161 ± 0.000	0.013 ± 0.016	0.035 ± 0.017	0.010 ± 0.015	0.003 ± 0.010
	J	0.766 ± 0.011	0.826 ± 0.010	0.824 ± 0.039	0.852 ± 0.016	0.933 ± 0.008
	τ_K	0.661 ± 0.016	0.831 ± 0.006	0.846 ± 0.014	0.872 ± 0.020	0.932 ± 0.006
Words	$\Delta \langle k_s \rangle$	0.118 ± 0.000	0.105 ± 0.000	0.108 ± 0.000	0.107 ± 0.000	0.102 ± 0.000
	ΔD	0.552 ± 0.010	0.484 ± 0.000	0.458 ± 0.013	0.097 ± 0.000	0.032 ± 0.000
	J	0.473 ± 0.003	0.575 ± 0.001	0.575 ± 0.002	0.592 ± 0.001	0.675 ± 0.002
	τ_K	0.668 ± 0.003	0.740 ± 0.001	0.758 ± 0.003	0.794 ± 0.003	0.815 ± 0.001
Cookpad – Greece	$\Delta \langle k_s \rangle$	0.002 ± 0.000	0.001 ± 0.000	0.002 ± 0.000	0.002 ± 0.001	0.000 ± 0.000
	ΔD	0.110 ± 0.003	0.113 ± 0.007	0.129 ± 0.003	0.016 ± 0.006	0.004 ± 0.003
	J	0.846 ± 0.003	0.865 ± 0.003	0.892 ± 0.004	0.941 ± 0.002	0.964 ± 0.002
	τ_K	0.850 ± 0.001	0.871 ± 0.001	0.894 ± 0.001	0.943 ± 0.002	0.968 ± 0.004
Cookpad – Spain	$\Delta \langle k_s \rangle$	0.002 ± 0.000	0.005 ± 0.000	0.005 ± 0.000	0.002 ± 0.000	0.002 ± 0.000
	ΔD	0.240 ± 0.006	0.346 ± 0.006	0.362 ± 0.005	0.238 ± 0.005	0.234 ± 0.006
	J	0.762 ± 0.006	0.872 ± 0.004	0.903 ± 0.003	0.760 ± 0.005	0.762 ± 0.006
	τ_K	0.837 ± 0.001	0.890 ± 0.001	0.907 ± 0.000	0.837 ± 0.001	0.837 ± 0.001
Cookpad – UK	$\Delta \langle k_s \rangle$	0.001 ± 0.001	0.005 ± 0.001	0.012 ± 0.001	0.001 ± 0.001	0.001 ± 0.000
	ΔD	0.030 ± 0.014	0.027 ± 0.016	0.085 ± 0.012	0.076 ± 0.015	0.012 ± 0.015
	J	0.754 ± 0.010	0.781 ± 0.007	0.827 ± 0.005	0.835 ± 0.003	0.886 ± 0.006
	τ_K	0.826 ± 0.003	0.852 ± 0.003	0.893 ± 0.002	0.886 ± 0.002	0.922 ± 0.002

Supplementary Table S1: Average and standard deviation of the four indicators characterising the k -core decomposition. In the cells with missing values, the shuffling method did not converge.



Supplementary Figure S2: Graphical summary of the values reported in Supplementary Table S1. For each pair of an empirical network and indicator, we show the value of the indicator for each shuffling method. The error bars represent the standard deviation.

2 Effects of changing the resolution of the Louvain method

A pitfall of the Louvain method is its propensity to merge small communities due to the existence of a lower bound in the size of the communities (*i.e.*, the modularity’s resolution limit) [1, 2]. However, communities of empirical networks may not have a typical size, and small communities coexist with large ones in general. A method for mitigating the resolution limit is to introduce a resolution parameter $r \in (0, 1]$ into the Louvain algorithm [3]. By tuning r , it is possible to vary the resolution scale of the detected communities, spanning from large (*i.e.*, $r \sim 1$) to small (*i.e.*, $r \sim 0$) communities. We denote the Louvain method using a different resolution r by L_{vnR} .

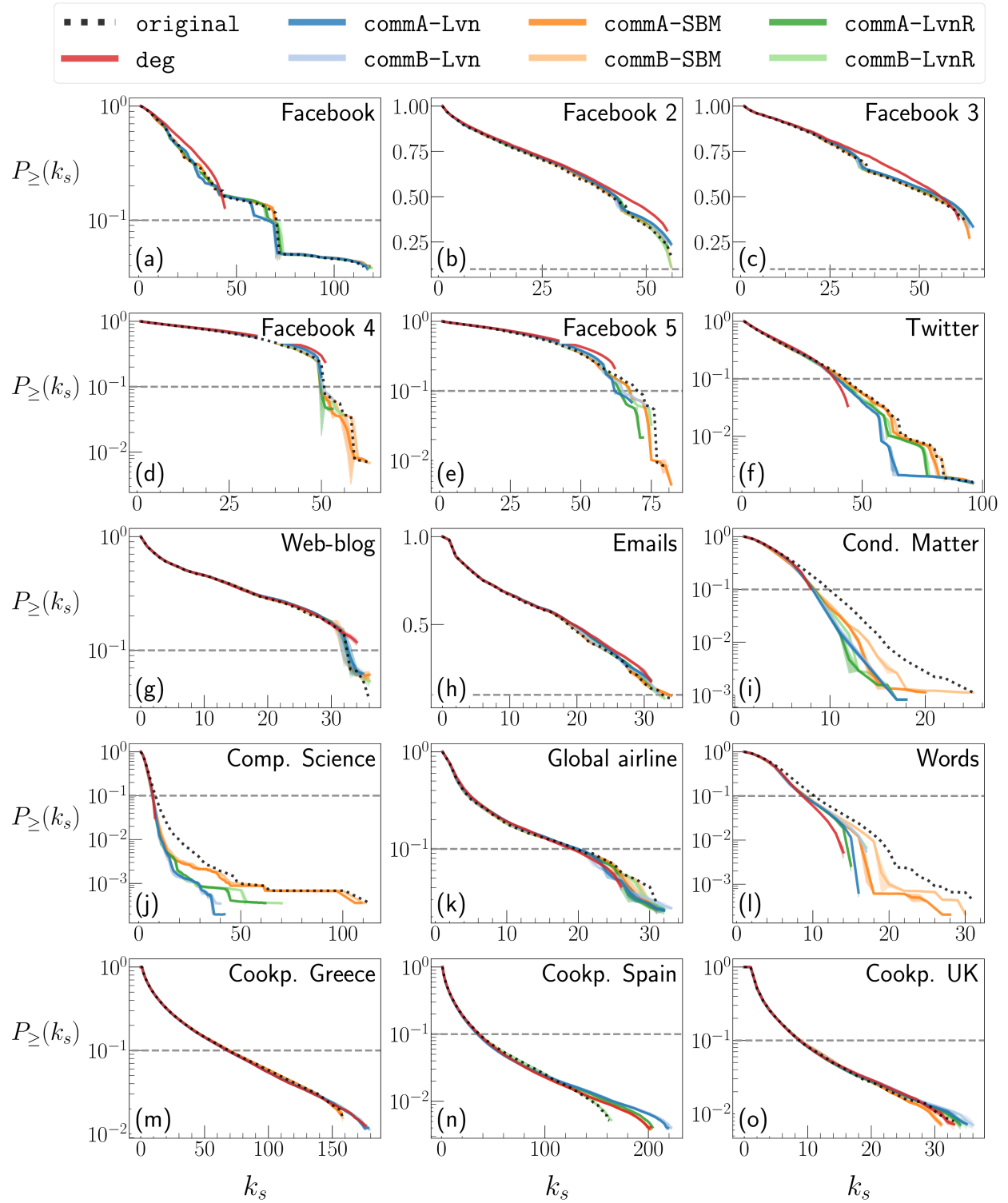
Figure 2 in the main text shows that commB combined with the communities found by the SBM reproduces the tail of $P_{\geq}(k_s)$ of the empirical networks most accurately. Table 1 indicates that SBM tends to find more communities than L_{vn} , although there are exceptions. To understand whether the different number of communities found by SBM and L_{vn} is the reason behind their different performances, we extracted the communities using L_{vnR} with $r \in \{0.1, 0.3, 0.5\}$. For the sake of brevity, we only discuss the results for $r = 0.3$ in the following text. However, we have verified that the results for the other values of r are similar.

In Supplementary Table S2 we show, for all the data sets considered, the number of communities, N_c , and the modularity, Q , corresponding to the community structure found using L_{vn} , SBM, and L_{vnR} with $r = 0.3$. With L_{vnR} , the number of communities is similar or even larger than that obtained with SBM. Supplementary Figures S3 and S4 show $P_{\geq}(k_s)$ plotted against k_s and the four indicators used for comparing the innermost k -shells, respectively, including the results obtained with L_{vnR} . These figures indicate that using $r = 0.3$ as opposed to $r = 1$ improves the ability of the Louvain algorithm to mimic the structure of the k -shell. In Supplementary Fig. S5 we summarise the performances of the different shuffling methods including L_{vnR} .

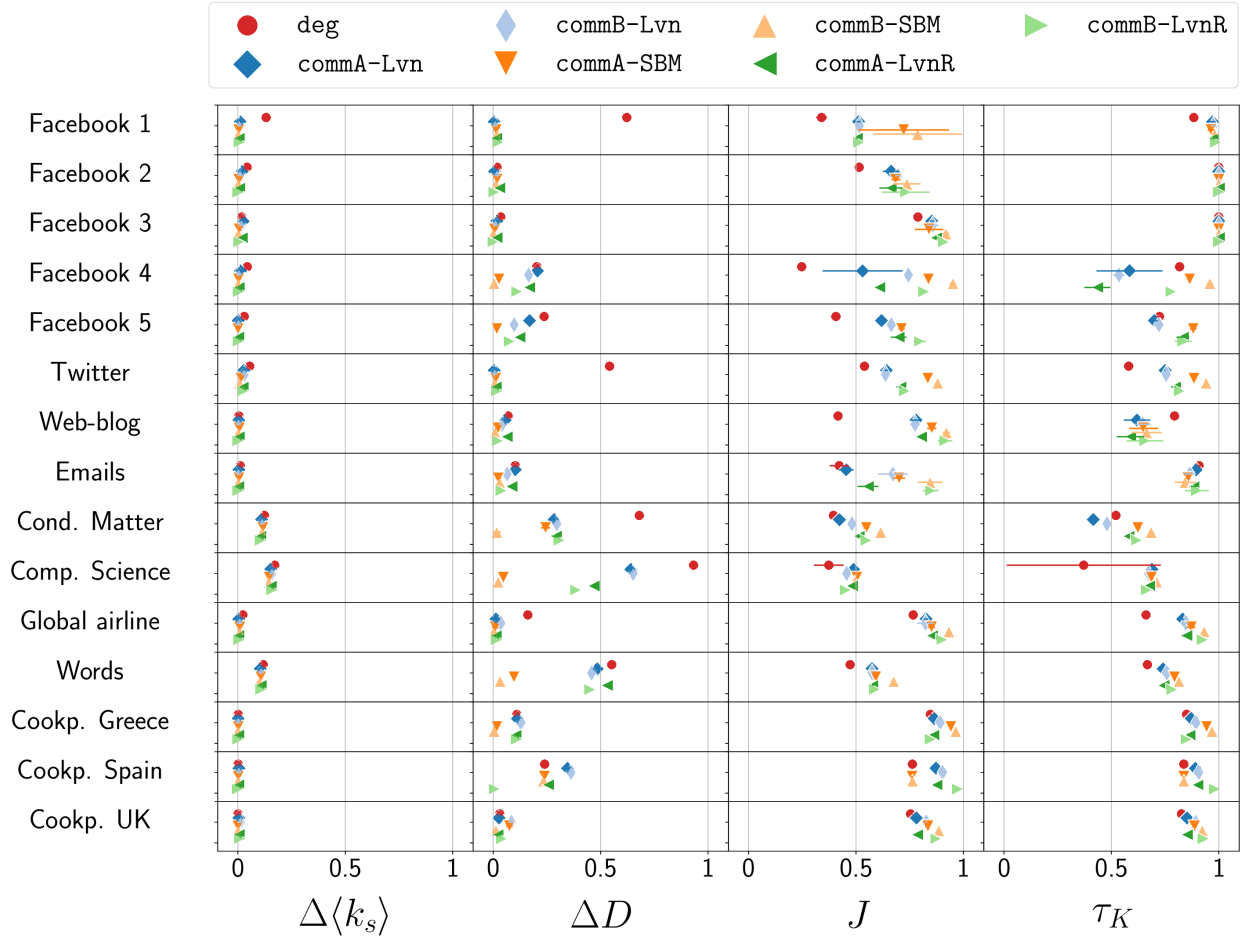
Although L_{vnR} mimics the k -shell features better than SBM for some data sets and indicators (approximately around the 20% of the cases), SBM still attains the highest success ratio for each indicator, f_X . The few cases for which commB-L_{vnR} does better than commB-SBM are the networks for which the difference between the empirical $P_{\geq}(k_s)$ and $P_{\geq}(k_s)$ obtained from the deg shuffling apparently looks small, such as the Emails and Cookpad UK networks. In these networks, the differences between the $P_{\geq}(k_s)$ of the networks obtained using commB-L_{vnR} and commB-SBM are also small. By contrast, other data sets such as Condensed Matter, Computer Science, and Words show bigger differences between their $P_{\geq}(k_s)$ and that obtained using the deg method. In these data sets, commB-SBM is much better than commB-L_{vnR} , although commB-L_{vnR} is better than commB-L_{vn} . Overall, these results suggest that the increase in the number of communities enabled by a small r does not lead to reconstruction of the k -shell structure with a better accuracy than SBM does.

Data set	$N_c^{L_{vn}}$	$Q^{L_{vn}}$	N_c^{SBM}	Q^{SBM}	$N_c^{L_{vnR}}$	$Q^{L_{vnR}}$
Facebook 1	16	0.835	62	0.551	29	0.819
Facebook 2	19	0.419	198	0.158	67	0.348
Facebook 3	8	0.436	87	0.139	36	0.294
Facebook 4	10	0.438	274	0.193	72	0.381
Facebook 5	18	0.470	547	0.172	92	0.417
Twitter	73	0.808	510	0.511	136	0.779
Web-blogs	275	0.426	17	0.076	331	0.150
Emails	26	0.410	33	0.232	61	0.350
Cond. Matter	619	0.730	203	0.633	716	0.718
Comp. Science	209	0.822	676	0.726	438	0.812
Global airline	26	0.665	40	0.311	55	0.542
Words	378	0.759	548	0.583	523	0.747
Cookpad Greece	40	0.166	76	0.020	365	0.067
Cookpad Spain	262	0.270	90	0.035	501	0.164
Cookpad UK	199	0.350	8	0.114	320	0.314

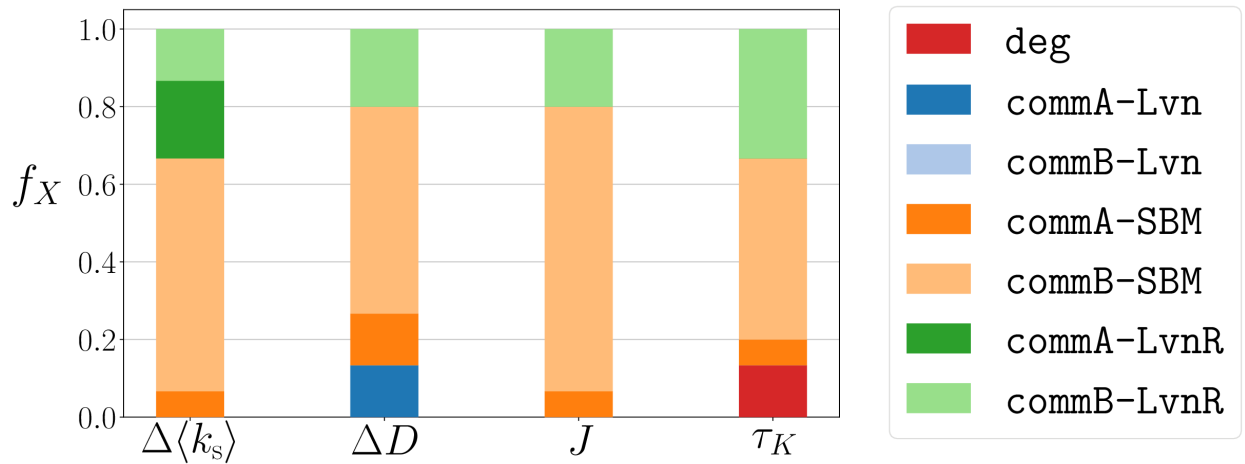
Supplementary Table S2: Summary of the properties of the community structures of the data sets analysed using different community detection methods. For each pair (network, method) we computed the number of communities, N_c , and the value of the modularity Q . Each pair of columns accounts for a different method, namely: Louvain (L_{vn}), stochastic block model (SBM), and Louvain with a resolution parameter $r = 0.3$ (L_{vnR}).



Supplementary Figure S3: Survival function of the probability distribution of the k -shell index, $P_{\ge}(k_s)$, as a function of k_s for all the cases considered in Fig. 1 plus the cases in which we identify communities using the Louvain method with a resolution parameter of $r = 0.3$. See the caption or Supplementary Fig. S1 for notations and legends.



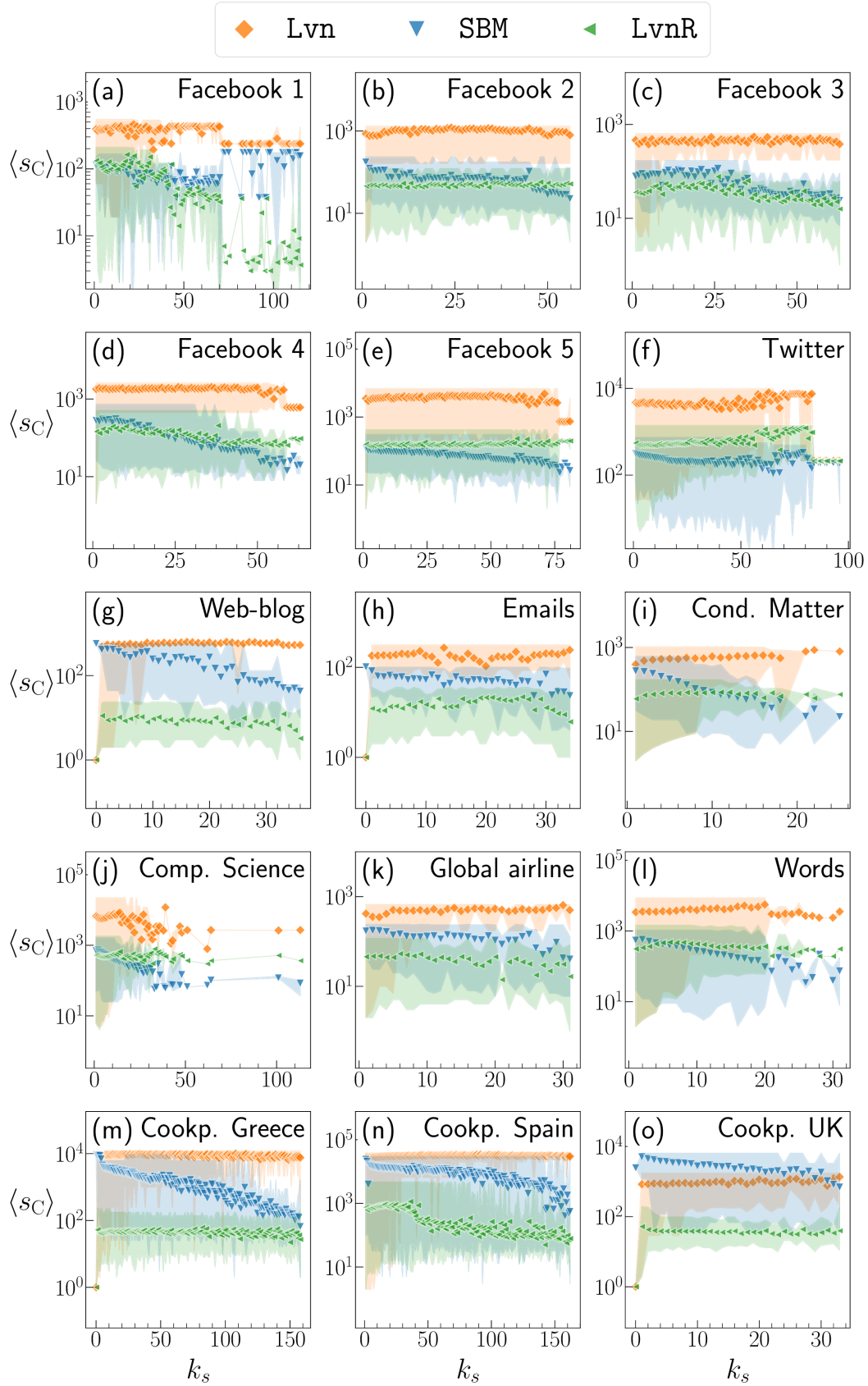
Supplementary Figure S4: Graphical summary of the average and standard deviation of the four indicators characterising the k -core decomposition. In addition to the information displayed in Supplementary Fig. S2, we consider the community structure detected by the Louvain method with $r = 0.3$ (LvnR). See the caption or Supplementary Fig. S2 for notations and legends.



Supplementary Figure S5: Summary of the performances of the different shuffling methods in reproducing the features of the k -shells according to four indicators. We report the fraction of data sets for which a given combination of the shuffling method and the community detection method yields an indicator's value closest to that for the original network. In addition to the methods considered in Fig. 2, we also consider the case of the communities extracted using the Louvain method with $r = 0.3$. See the caption or Fig. 2 for notations and legends.

To investigate which features of the SBM and Louvain algorithms are responsible for the difference in their performances, we study the average of the size of the communities to which nodes of a certain k -shell belong, $\langle s_C \rangle$, as a function of the k -shell index, k_s . In Supplementary Fig. S6, we observe how $\langle s_C \rangle$ of the communities found by the Louvain method (LVN) stays nearly constant across the entire range of k_s values. By contrast, with SBM, $\langle s_C \rangle$ monotonically decreases as k_s increases, such that nodes in inner k -shells tend to belong to smaller communities. Although a high resolution (*i.e.*, a small r value) in the Louvain method produces a large number of communities (see Supplementary Table S2), the behaviour of $\langle s_C \rangle$ for LVN and LVNR is similar, with the major difference that the value of $\langle s_C \rangle$ is smaller for LVNR.

These results altogether lead us to conclude that our method combined with the community structure identified using the Louvain method with a higher resolution does not outperform our method combined with SBM in grasping the features of the k -core decomposition. This may be because SBM is capable of finding more universal mesostructures than those found by the Louvain method [4–6].



Supplementary Figure S6: Average size of the communities to which the nodes having k -shell index k_s belong to, $\langle s_C \rangle$, versus k_s . We identify the community structure using either the Louvain (Lvn), the stochastic block model (SBM), or the Louvain with higher resolution (LvnR) methods. The resolution parameter for (LvnR) is equal to $r = 0.3$. Shaded areas denote the standard deviation. Each panel accounts for a different data set.

3 The LFR model

The Lancichinetti-Fortunato-Radicchi (LFR) model generates networks where both the node’s degree and the size of the communities (*i.e.*, the number of nodes belonging to a community) follow power-law distributions [7]. Such features are found in many empirical networks [8] and have led to the success of the LFR model as generator of benchmark networks to test community detection algorithms [2]. A main finding presented in the main text is that preserving the community structure of the original network in addition to the degree of each node improves the ability of the shuffling methods to mimic the k -core decomposition of the original networks. Here, to test whether or not the community structure and the degree of each node, but not a possible intricate association between the two, is sufficient for mimicking the features of k -core decomposition observed for many empirical networks, we generated networks using the LFR model and analysed their k -cores and those of the shuffled counterparts.

The LFR algorithm depends on the following parameters: the exponent, $t_1 \in [2, 3]$, of the degree distribution $P(k) \propto k^{-t_1}$; the exponent, $t_2 \in [1, 2]$, of the community’s size distribution $P(S_c) \propto S_c^{-t_2}$; the mixing parameter, $\mu \in [0, 1]$, specifying the fraction of intra-community edges for a node. A value of $\mu = 0$ indicates that a node is connected only with nodes belonging to communities different from its own. A value of $\mu = 1$ indicates that a node is connected exclusively with nodes belonging to its own community; either one of the following: the average degree, $\langle k \rangle$, the minimum degree, k_{\min} , or the minimum number of communities, $\min N_c$. This stochastic algorithm may not produce a network fulfilling all the requirements in some realisations. Therefore, we have to set the parameter values to ensure the algorithm’s convergence.

To encompass a good spectrum of networks, we consider four batches of parameter sets, which are summarised in Supplementary Table S3, together with the properties of the generated networks. Each batch of parameter sets consists of a value of t_1 , a value of t_2 , and seven values of μ ranging from 0.1 to 0.8. We assumed $N = 10000$ nodes and used the implementation of the LFR algorithm in the NetworkX Python package [9].

For each network generated, we extracted its k -core decomposition and calculated the four indicators. We did the same for the shuffled counterparts generated using the `deg`, `commA`, and `commB` methods. In analogy to Supplementary Fig. S1, in Supplementary Figs. S7–S10 we show the survival function of the probability distribution of the k -shell index, $P_{\geq}(k_s)$, for the original LFR networks and the shuffled counterparts, one figure per each (t_1, t_2) pair. An eye inspection of Supplementary Figs. S7–S10 highlights the existence of three trends.

First, Supplementary Figs. S7 and S8 indicate that, in networks generated using the smaller t_1 values (*i.e.*, parameters batches 1 and 2 in Supplementary Table S3), the shuffled networks generated by `deg`, `commA-LvN`, and `commB-LvN` attain a k -core decomposition with a degeneracy, D , considerably higher than the original one. In contrast, Supplementary Figs. S9 and S10 indicate that, with the larger t_1 values (*i.e.*, parameter batches 3 and 4), we recover the same trend as that shown in Fig. 1. In other words, D for the original networks are larger than that for the shuffled networks. The difference between the original D and its shuffled counterpart seems to be influenced by the value of t_1 , but not t_2 or μ .

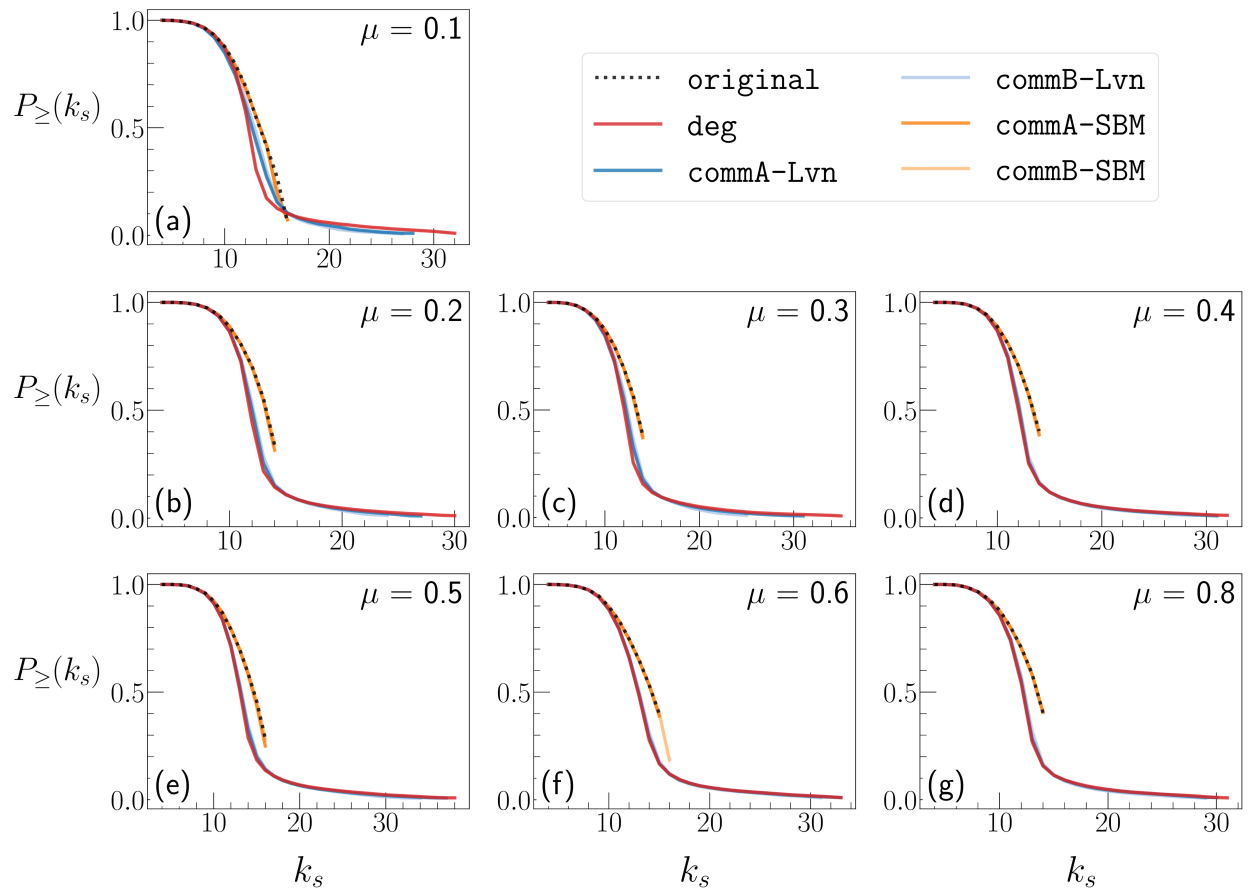
Second, $P_{\geq}(k_s)$ for the original LFR networks mainly decreases smoothly as k_s increases, without plateaus or abrupt drops. Therefore, the k -core decomposition of LFR networks does not return any k -shell that is empty or much more populated than its adjacent k -shells. This result is in stark contrast to that for various empirical networks, *e.g.*, the Facebook 1 data set (see Supplementary Fig. S1).

Third, regardless of the values of t_1 , t_2 , and μ , the `commB-SEB` shuffling method produces networks with the $P_{\geq}(k_s)$ more akin to the original one than the other shuffling methods do. This result is consistent with that for the empirical networks presented in the main text.

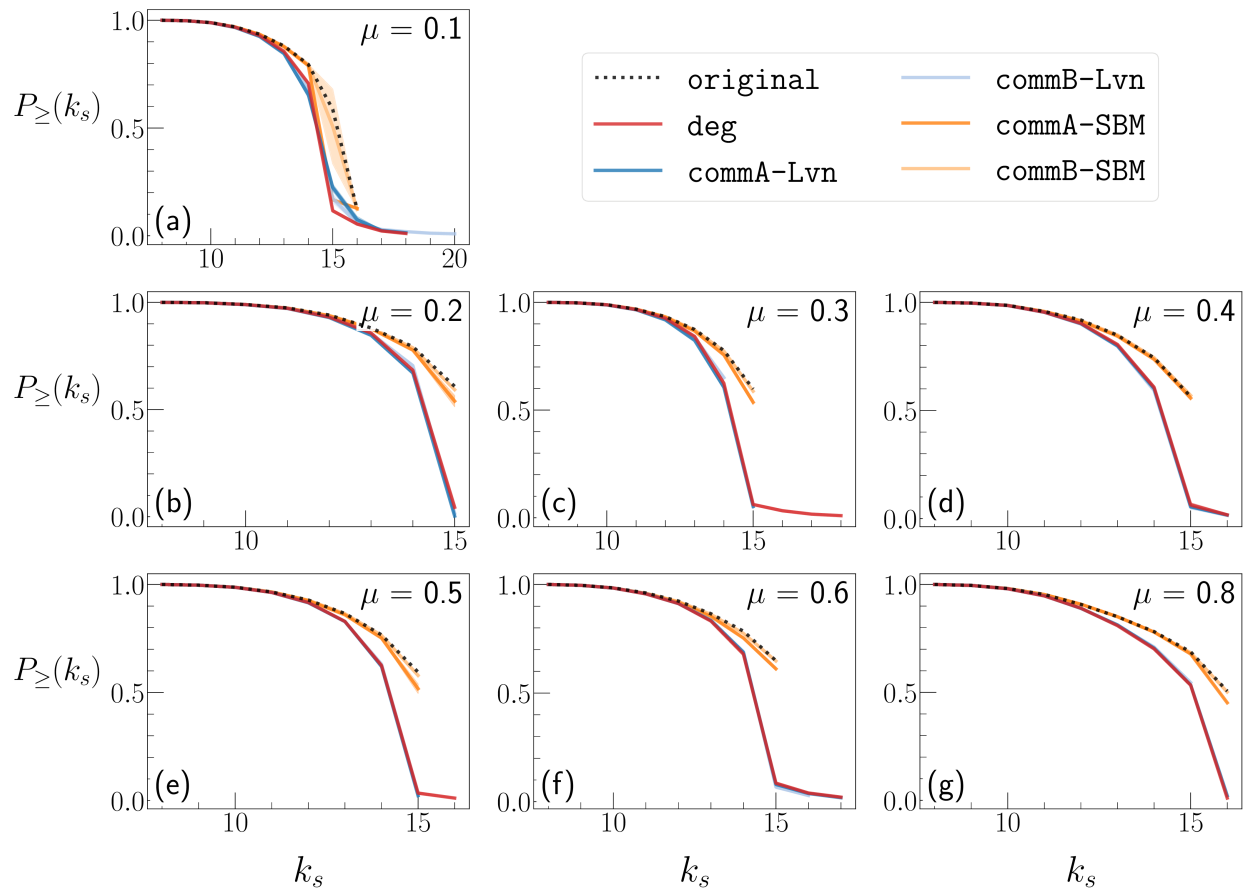
In a nutshell, the analysis of the k -core decomposition of networks generated by the LFR model reveals that the presence of communities is not enough to justify main properties of the k -shell structure observed in the empirical networks.

LFR parameters		L	k_{\min}	$\langle k \rangle$	k_{\max}	$\langle k_s \rangle$	D	N_c^{Lvn}	Q^{Lvn}	N_c^{SBM}	Q^{SBM}
t_1, t_2	μ										
Parameter batch 1											
$t_1 = 2.2$ $t_2 = 1.5$	0.1	120893	4	24.179	3470	12.541	16	10	0.673	29	0.041
	0.2	116200	4	23.240	3380	12.201	14	4	0.497	16	-0.006
	0.3	118260	4	23.652	3199	12.188	14	7	0.458	26	-0.002
	0.4	118547	4	23.709	6309	12.287	14	7	0.234	19	-0.053
	0.5	130304	4	26.061	4481	12.548	16	7	0.250	24	-0.038
	0.6	126277	4	25.255	4607	12.967	15	10	0.164	8	-0.151
	0.8	118032	4	23.606	4028	12.263	14	10	0.162	5	-0.156
Parameter batch 2											
$t_1 = 2.6$ $t_2 = 2.0$	0.1	132920	8	26.584	2474	14.277	16	5	0.651	16	0.118
	0.2	129069	8	25.814	1641	14.186	15	8	0.595	22	0.139
	0.3	129024	8	25.805	1287	14.138	15	9	0.487	26	0.091
	0.4	128606	8	25.721	3305	14.015	15	7	0.222	9	-0.020
	0.5	127596	8	25.519	1504	14.105	15	8	0.227	20	0.041
	0.6	131024	8	26.205	1287	14.165	15	7	0.178	5	-0.093
	0.8	133017	8	26.603	4436	14.665	16	8	0.166	8	-0.087
Parameter batch 3											
$t_1 = 2.9$ $t_2 = 1.5$	0.1	315105	24	63.012	4249	35.907	37	4	0.511	14	0.115
	0.2	320836	24	64.167	2439	36.362	37	12	0.584	31	0.179
	0.3	319482	24	63.896	3732	36.234	37	10	0.359	29	0.078
	0.4	319070	24	63.814	2371	36.102	37	11	0.314	30	0.063
	0.5	321222	24	64.244	2795	36.816	38	9	0.204	27	0.029
	0.6	317738	24	63.548	2371	36.019	37	8	0.146	18	0.016
	0.8	305945	24	61.189	2246	35.049	36	9	0.109	4	-0.052
Parameter batch 4											
$t_1 = 3.0$ $t_2 = 2.0$	0.1	247311	20	49.462	2819	28.561	31	31	0.740	57	0.323
	0.2	246506	20	49.301	1228	27.691	28	40	0.651	69	0.331
	0.3	254822	20	50.964	1779	29.468	30	29	0.484	50	0.224
	0.4	249528	20	49.906	1131	28.457	29	37	0.387	71	0.156
	0.5	254371	20	50.874	2668	29.120	30	17	0.211	42	0.070
	0.6	243746	20	48.749	1097	28.311	29	20	0.186	50	0.073
	0.8	251094	20	50.219	3569	28.364	29	9	0.119	4	-0.053

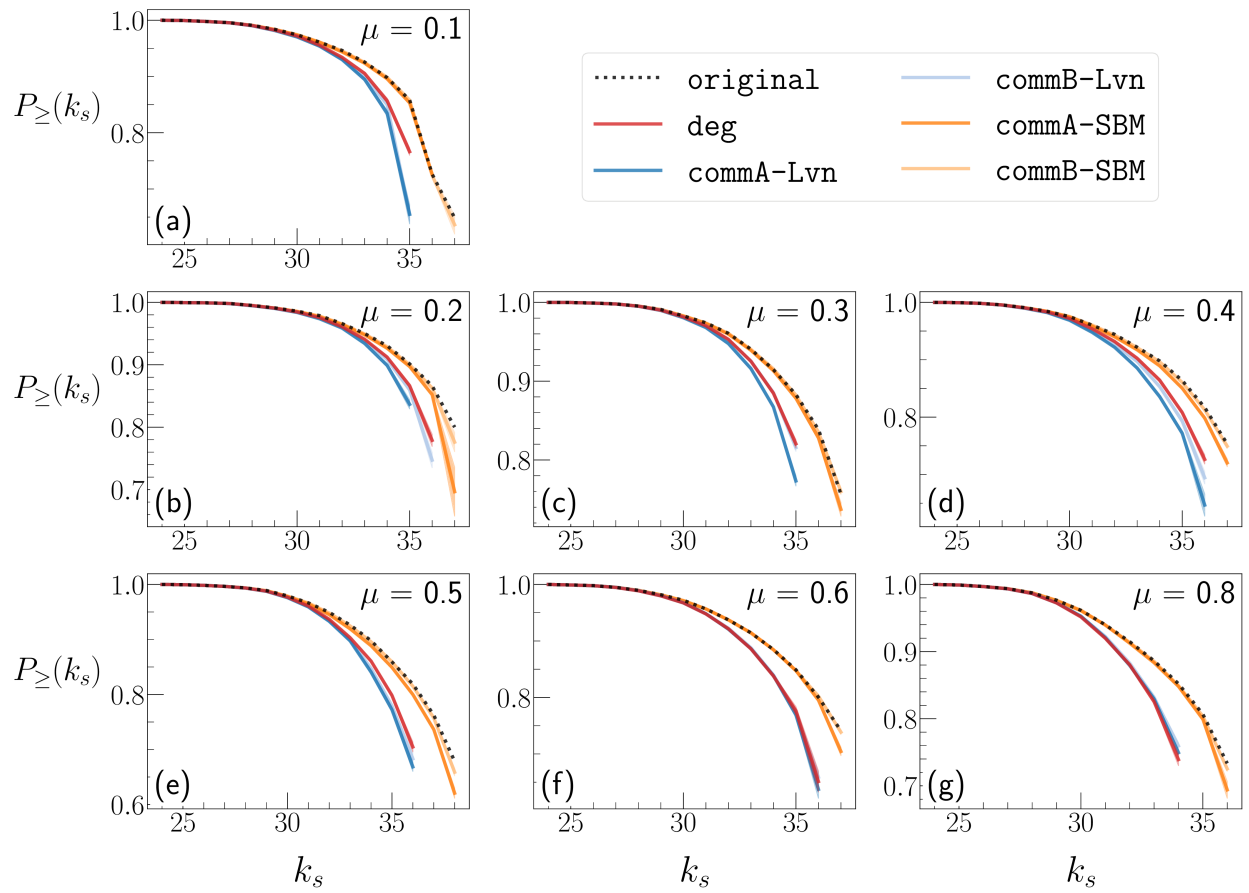
Supplementary Table S3: Summary of the properties of the networks generated with the LFR model. For each combination of parameters t_1 , t_2 , and μ we report the number of edges, L , minimum degree, k_{\min} , average degree, $\langle k \rangle$, maximum degree, k_{\max} , degeneracy, D , number of communities, N_c , and modularity, Q , for communities extracted using either the Louvain (Lvn) or stochastic block model (SBM) method. All networks have $N = 10000$ nodes.

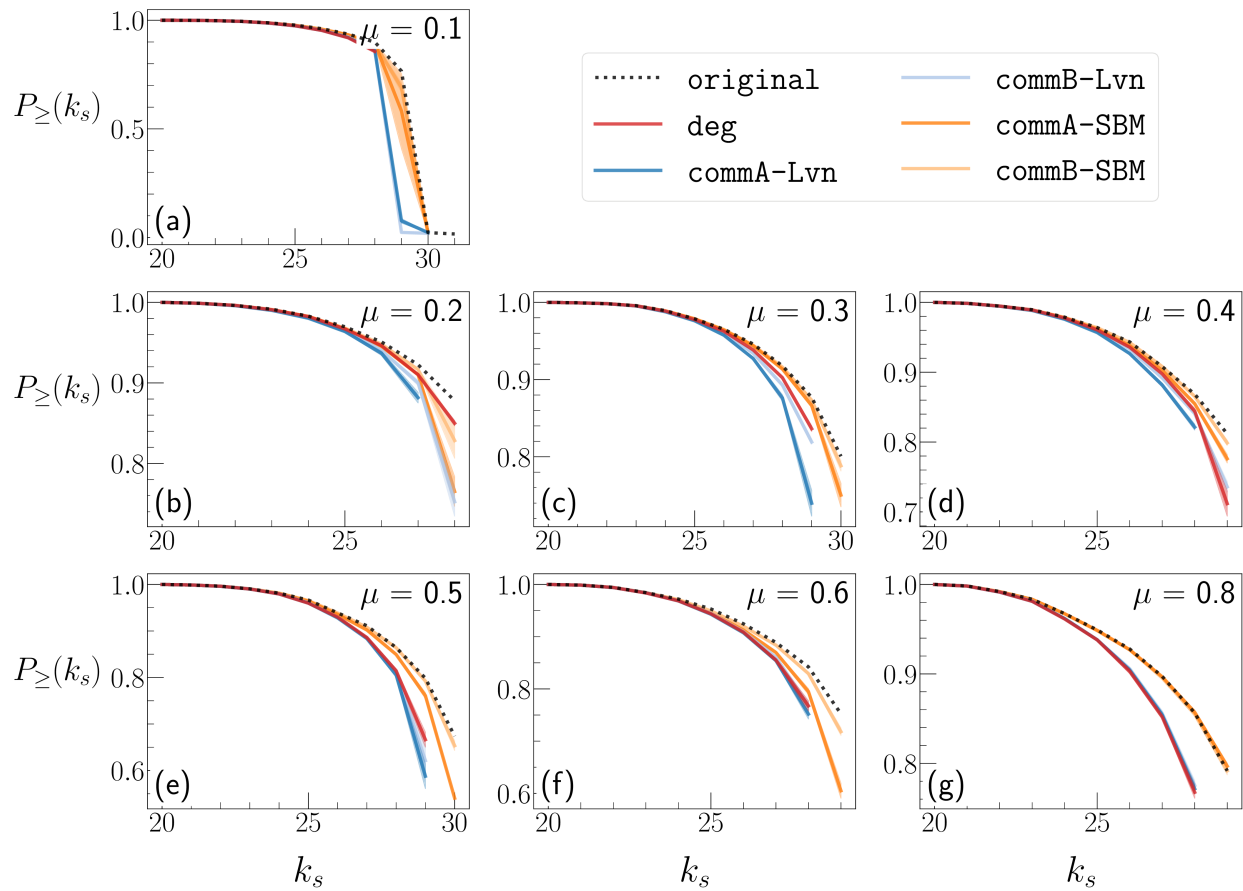


Supplementary Figure S7: Survival function of the probability distribution, $P_{\ge}(k_s)$, of the k -shell index, k_s , for the LFR networks generated using parameter batch 1 (*i.e.*, with $t_1 = 2.2$ and $t_2 = 1.5$; see Supplementary Table S3). The dotted lines correspond to the original network. The solid lines correspond to shuffled networks. Each panel corresponds to a value of μ . Shuffled results are averages over 10 realisations. The shaded area corresponds to the standard deviation. All networks have $N = 10000$ nodes.



Supplementary Figure S8: Survival function of the probability distribution, $P_{\ge}(k_s)$, of the k -shell index, k_s , for the LFR networks generated using parameter batch 2 (*i.e.*, with $t_1 = 2.6$ and $t_2 = 2.0$; see Supplementary Table S3). See the caption or Supplementary Fig. S7 for notations and legends.





Supplementary Figure S10: Survival function of the probability distribution, $P_{\ge}(k_s)$, of the k -shell index, k_s , for the LFR networks generated using parameter batch 4 (*i.e.*, with $t_1 = 3.0$ and $t_2 = 2.0$; see Supplementary Table S3). See the caption or Supplementary Fig. S7 for notations and legends.

4 Relationship between community structure and k -core decomposition

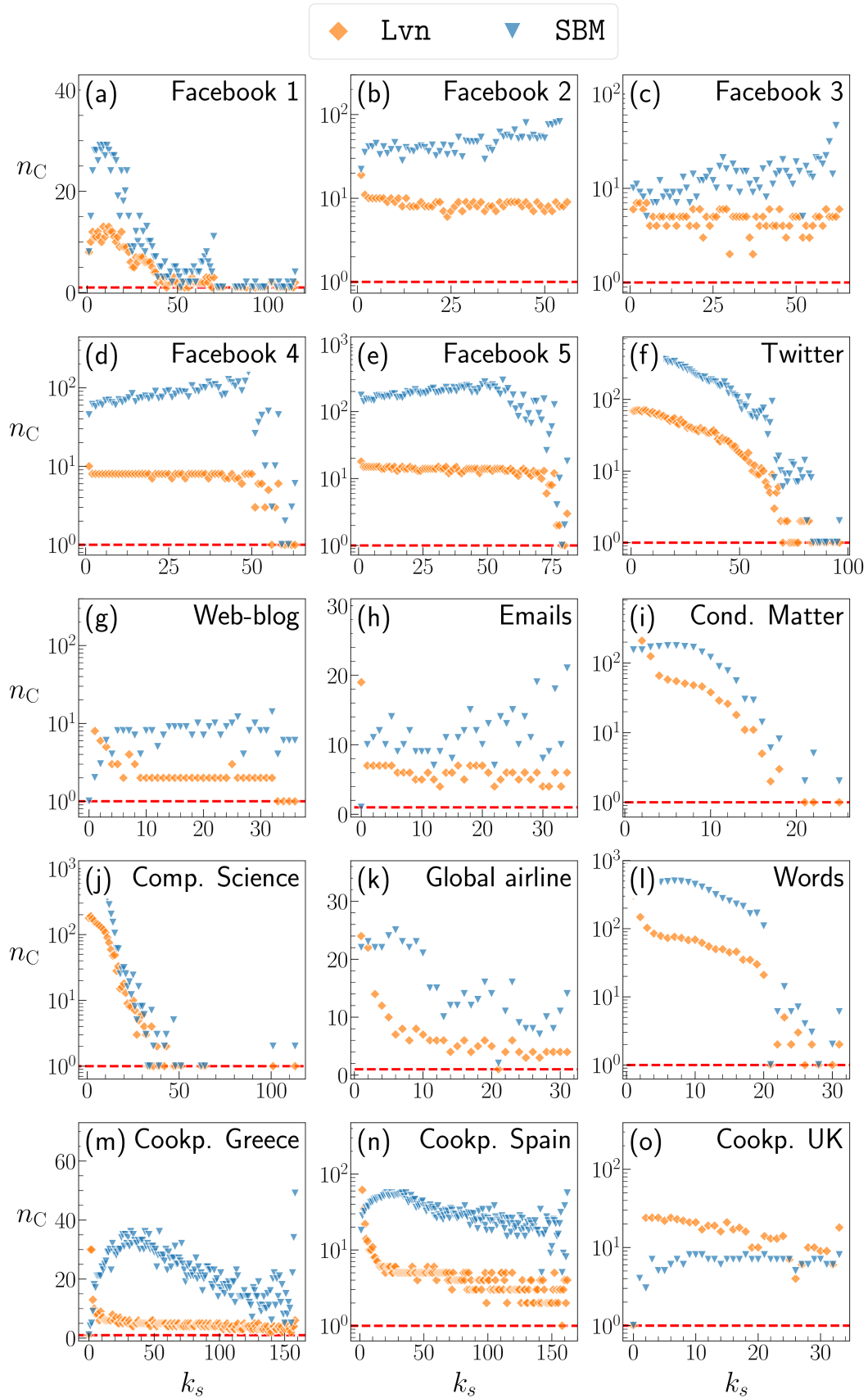
In this section, we examine the number of communities to which the nodes in each k -shell belong, with the aim of examining whether or not those nodes are concentrated into one or a small number of communities, particularly for nodes in innermost k -shells. This analysis is similar to Supplementary Fig. S6, whereas in that case we focused on the averaged community size. Supplementary Figure S11 shows the number of distinct communities to which the nodes with a given k_s value belong, denoted by $n_C(k_s)$, for all the data sets. In agreement with Fig. 3, some data sets show a strong concentration of the innermost k -shells (*i.e.*, nodes with large k_s values) into one or a few communities.

Next, we ask whether or not the number of communities across which each k -shell is distributed is a byproduct of random interactions. To answer this question, first, for each network, we extract communities using either L_{VN} or SBM. Second, we compute $n_C(k_s)$ for each k_s . Third, we compute the same quantity for the case in which we permute the association between the k -shell index of each node, $k_s(i)$, and the community membership of the node, $g(i)$, uniformly at random; in fact, it is sufficient to randomly permute either $\{k_s(1), \dots, k_s(N)\}$ or $\{g(1), \dots, g(N)\}$, not both. Fourth, we calculate the number of communities to which the set of nodes with a given k_s value belong after the permutation, which is denoted by $n_C^S(k_s)$. Fifth, using an approach similar to the calculation of the rich-club coefficient [10], we compute

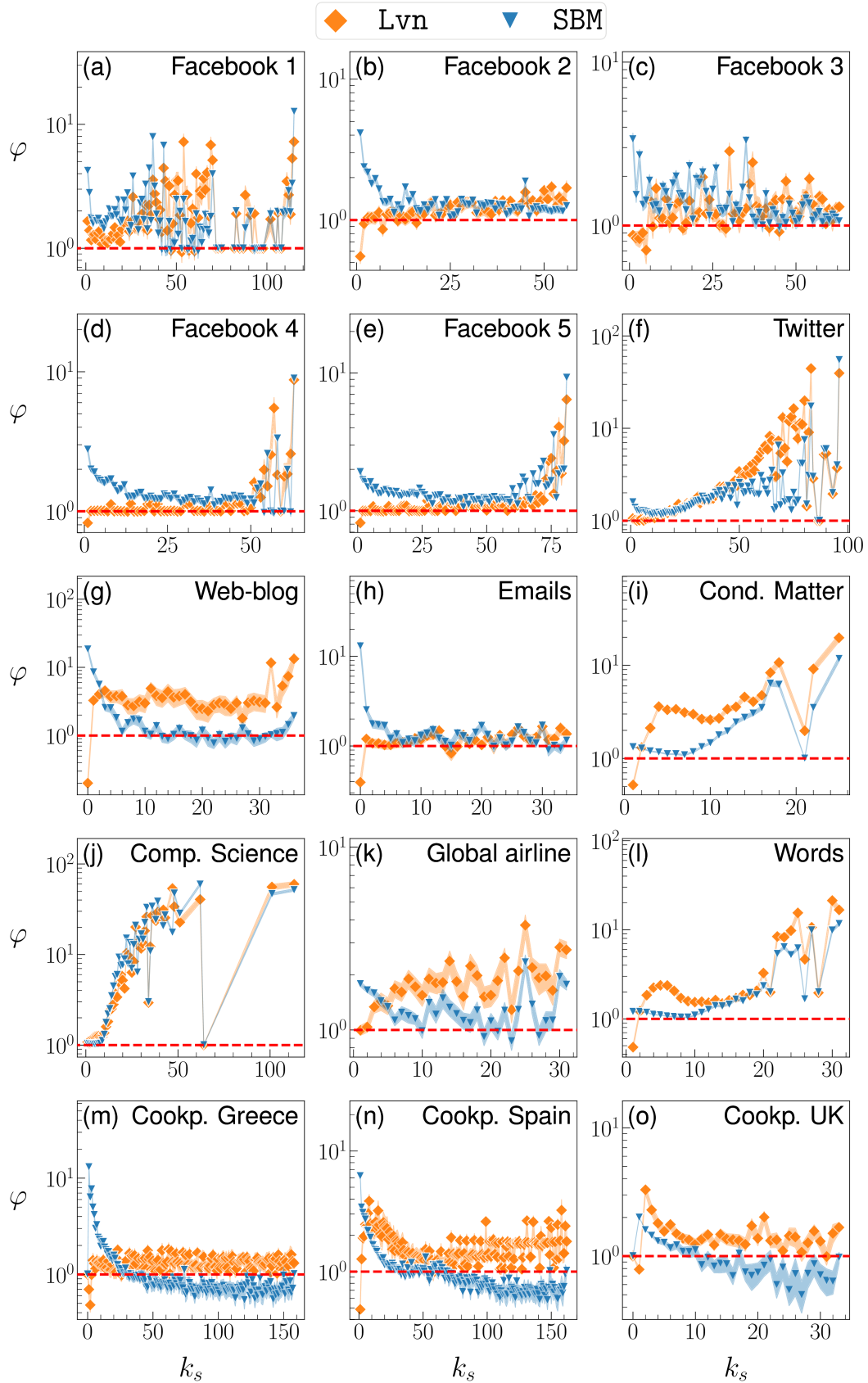
$$\varphi(k_s) = \frac{n_C^S(k_s)}{n_C(k_s)} \quad (\text{S1})$$

for each k_s . A value of $\varphi(k_s)$ larger (smaller) than 1 indicates that the number of communities to which the nodes having the k_s value belong is smaller (larger) than in the case of the randomised association between the nodes and communities. Therefore, $\varphi(k_s)$ larger than 1 implies that the nodes with the given k -shell index, k_s , are concentrated into a relatively small number of communities as compared to randomised counterparts.

In Supplementary Fig. S12 we plot $\varphi(k_s)$ against k_s for all the data sets. We observe that, with the exception of the Spanish and British Cookpad's networks, $\varphi(k_s)$ tends to be larger than 1. This result implies that, on average, nodes of a given k -shell tend to belong to less communities than the randomised case. We stress that the permutation of either the k -shell index or the community membership sequences may return networks whose k -shell and community structure are not physically plausible. For instance, if a node i receives a k -shell index value of α upon randomisation and α is larger than k_i (*i.e.*, degree of node i), then the node cannot belong to the corresponding k -shell.



Supplementary Figure S11: Number of communities, $n_C(k_s)$, to which the nodes having k -shell index k_s belong. The horizontal line is a guide to the eyes representing $n_C(k_s) = 1$. We identified the community structure using either Lvn or SBM. Each panel accounts for a different data set.



Supplementary Figure S12: Ratio, $\varphi(k_s)$, (see (S1)) plotted against the k -shell index, k_s , for all the data sets. We identified the community structure using either L_{vn} or SBM . Each panel accounts for a different data set. Results are averaged over one hundred runs of randomisation between the association between the node's k -shell index and community label. The horizontal dashed lines represent $\varphi(k_s) = 1$.

References

- [1] Fortunato, S. & Barthélemy, M. Resolution limit in community detection. *Proceedings of the National Academy of Sciences of the United States of America* **104**, 36–41, DOI: 10.1073/pnas.0605965104 (2007).
- [2] Fortunato, S. & Hric, D. Community detection in networks: A user guide. *Physics Reports* **659**, 1–44, DOI: 10.1016/j.physrep.2016.09.002 (2016).
- [3] Lambiotte, R., Delvenne, J. C. & Barahona, M. Random walks, Markov processes and the multiscale modular organization of complex networks. *IEEE Transactions on Network Science and Engineering* **1**, 76–90, DOI: 10.1109/TNSE.2015.2391998 (2014).
- [4] Olhede, S. C. & Wolfe, P. J. Network histograms and universality of blockmodel approximation. *Proceedings of the National Academy of Sciences of the United States of America* **111**, 14722–14727, DOI: 10.1073/pnas.1400374111 (2014).
- [5] Newman, M. E. J. Equivalence between modularity optimization and maximum likelihood methods for community detection. *Phys. Rev. E* **94**, 052315, DOI: 10.1103/PhysRevE.94.052315 (2016).
- [6] Young, J.-G., St-Onge, G., Desrosiers, P. & Dubé, L. J. Universality of the stochastic block model. *Phys. Rev. E* **98**, 032309, DOI: 10.1103/PhysRevE.98.032309 (2018).
- [7] Lancichinetti, A., Fortunato, S. & Radicchi, F. Benchmark graphs for testing community detection algorithms. *Physical Review E* **78**, 046110, DOI: 10.1103/PhysRevE.78.046110 (2008).
- [8] Amaral, L. A. N., Scala, A., Barthelemy, M. & Stanley, H. E. Classes of small-world networks. *Proceedings of the National Academy of Sciences of the United States of America* **97**, 11149–11152, DOI: 10.1073/pnas.200327197 (2000).
- [9] Hagberg, A. A., Schult, D. A. & Swart, P. J. Exploring network structure, dynamics, and function using networkx. In Varoquaux, G., Vaught, T. & Millman, J. (eds.) *Proceedings of the 7th Python in Science Conference*, 11 – 15 (Pasadena, CA USA, 2008).
- [10] Colizza, V., Flammini, A., Serrano, M. Á. & Vespignani, A. Detecting rich-club ordering in complex networks. *Nature Physics* **2**, 110–115, DOI: 10.1038/nphys209 (2006).